行）に伴って血中HGF値は上昇し，回復時にはHGF値が減少する．また再発例，転移例においては更に高い値を示し，特に乳癌において転移が肝臓に起こった場合は，血中HGFの上昇が顕著にみられる．大腸癌，乳癌などでは血中HGF値に病理像との関連も認められ癌の重症度をよく反映しているといえる[4]．

9）その他の疾患

HGF値の報告は，ここ数年でこれまで研究が盛んであった主要臓器以外の疾患や，我々万人に身近な生活習慣病においても相次いでなされている．更に血液以外の滲出液の変化を知ることは傷害を把握するうえでより直接的であると考えられる．アミロイドーシスで血清HGF値は高値となり，特に1年生存率との間には負の相関がみられる．肥満では，脂肪細胞がHGFを産生することにより，血清HGF値とBMI（体格指数）の間に正の相関がみられている．また歯周病では歯肉溝液で，リウマチ性関節炎患者では関節液で，HGF値は高値を示す．

おわりに

これまでの様々な疾患モデル動物を用いた実験でのHGFによる治療効果の報告には目を見張るばかりである．傷害応答因子としてのHGFの血中動向を把握することは，傷害発生そのものを把握することに近い．HGFは様々な臓器障害に対して放出されるため傷害部位の特定には注意を要するが，他の検査を組み合わすことで傷害診断，疾病予後の予知に有効であると考えられる．

傷害時における血中HGFが活性化されているか否かの情報は，ある種の疾患にとっては有用であるが，c-Met側の傷害認知機構が明らかとなった今日ではHGF側の情報だけでは不十分であり検査感度的にも難しいことから，血中の総HGF量の値を知ることはこれまでと同様重要であろう．血中HGF値が変動する疾患の多くで，HGF，NK4の投与によりその症状が改善されることが動物レベルで明らかである．血中HGFの値を知ることで様々な疾病の早期診断の一助とし，HGF，NK4を治療薬として利用できる日ができるだけ早くくることを切に望む．

文献

1) Nakamura T, et al: Biochem Biophys Res Commun **122**: 1450-1459, 1984.
2) Nakamura T, et al: Nature **342**: 440-443, 1989.
3) 中村敏一，荻原俊男（監）：HGFの分子医学，メディカルレビュー社，1998.
4) Funakoshi H, Nakamura T: Clin Chim Acta **327**: 1-23, 2003.
5) Yamada A, et al: Biomed Res **16**: 105-114, 1995.
6) Onishi T, et al: J Immunol Methods **244**: 163-173, 2000.
7) Ido A, et al: Hepatol Res **30**: 175-181, 2004.
8) Hashigasako A, et al: J Biol Chem **279**: 26445-26452, 2004.
9) Matsumoto K, et al: Proc Natl Acad Sci USA **89**: 3800-3804, 1992.
10) 船越　洋，中村敏一：日本臨牀 **57**: 821-826, 1999.

Acta Neuropathol (2005) 110: 101–112
DOI 10.1007/s00401-005-1019-3

REGULAR PAPER

Shinsuke Kato · Masako Kato · Yasuko Abe
Tomohiro Matsumura · Takeshi Nishino · Masashi Aoki
Yasuto Itoyama · Kohtaro Asayama · Akira Awaya
Asao Hirano · Eisaku Ohama

Redox system expression in the motor neurons in amyotrophic lateral sclerosis (ALS): immunohistochemical studies on sporadic ALS, superoxide dismutase 1 (SOD1)-mutated familial ALS, and SOD1-mutated ALS animal models

Received: 21 September 2004 / Revised: 9 March 2005 / Accepted: 9 March 2005 / Published online: 28 June 2005
© Springer-Verlag 2005

Abstract Peroxiredoxin-II (PrxII) and glutathione peroxidase-I (GPxI) are regulators of the redox system that is one of the most crucial supporting systems in neurons. This system is an antioxidant enzyme defense system and is synchronously linked to other important cell supporting systems. To clarify the common self-survival mechanism of the residual motor neurons affected by amyotrophic lateral sclerosis (ALS), we examined motor neurons from 40 patients with sporadic ALS (SALS) and 5 patients with superoxide dismutase 1 (SOD1)-mutated familial ALS (FALS) from two different families (frameshift 126 mutation and A4 V) as well as four different strains of the SOD1-mutated ALS models (H46R/G93A rats and G1H/G1L-G93A mice). We investigated the immunohistochemical expression of PrxII/GPxI in motor neurons from the viewpoint of the redox system. In normal subjects, PrxII/GPxI immunoreactivity in the anterior horns of the normal spinal cords of humans, rats and mice was primarily identified in the neurons: cytoplasmic staining was observed in almost all of the motor neurons. Histologically, the number of spinal motor neurons in ALS decreased with disease progression. Immunohistochemically, the number of neurons negative for PrxII/GPxI increased with ALS disease progression. Some residual motor neurons coexpressing PrxII/GPxI were, however, observed throughout the clinical courses in some cases of SALS patients, SOD1-mutated FALS patients, and ALS animal models. In particular, motor neurons overexpressing PrxII/GPxI, i.e., neurons showing redox system up-regulation, were commonly evident during the clinical courses in ALS. For patients with SALS, motor neurons overexpressing PrxII/GPxI were present mainly within approximately 3 years after disease onset, and these overexpressing neurons thereafter decreased in number dramatically as the disease progressed. For SOD1-mutated FALS patients, like in SALS patients, certain residual motor neurons without inclusions also overexpressed PrxII/GPxI in the short-term-surviving FALS patients. In the ALS animal models, as in the human diseases, certain residual motor neurons showed overexpression of PrxII/GPxI during their clinical courses. At the terminal stage of ALS, however, a disruption of this common PrxII/GPxI-overexpression mechanism in neurons was observed. These findings lead us to the conclusion that the residual ALS neurons showing redox system up-regulation would be less susceptible to ALS stress and protect themselves from ALS neuronal death, whereas the breakdown of this redox system at the advanced disease stage accelerates neuronal degeneration and/or the process of neuronal death.

S. Kato (✉) · E. Ohama
Department of Neuropathology, Institute of Neurological Sciences, Faculty of Medicine, Tottori University, Nishi-cho 36-1, 683-8504 Yonago, Japan
E-mail: kato@grape.med.tottori-u.ac.jp
Tel.: +81-859-348034
Fax: +81-859-348289

M. Kato
Division of Pathology, Tottori University Hospital, Yonago, Japan

Y. Abe · T. Matsumura · T. Nishino
Department of Biochemistry and Molecular Biology, Nippon Medical School, Tokyo, Japan

M. Aoki · Y. Itoyama
Department of Neuroscience, Division of Neurology, Tohoku University Graduate School of Medicine, Sendai, Japan

K. Asayama
Department of Pediatrics, University of Occupational and Environmental Health, Kitakyushu, Japan

A. Awaya
Japan Science and Technology Agency, Tachikawa, Japan

A. Hirano
Division of Neuropathology, Department of Pathology, Montefiore Medical Center, Bronx, New York, USA

Keywords Amyotrophic lateral sclerosis · Peroxiredoxin-ll · Glutathione peroxidase-l · Redox system

Introduction

Amyotrophic lateral sclerosis (ALS), first described by Charcot and Joffroy in 1869 [11], is a fatal and age-associated neurodegenerative disorder that primarily involves both the upper and lower motor neurons [23]. This disease has been recognized as a distinct clinicopathological entity of unknown etiology for over 130 years.

During physiological processes and in response to external stimuli such as ultraviolet radiation, cells produce reactive oxygen species (ROSs). To protect itself from these potentially destructive ROSs, each cell of the living organs has developed a sophisticated antioxidant system. In such systems, there are two groups of the enzymes: those constituting the first group convert superoxide radicals into hydrogen peroxide (H_2O_2), and those of the second convert H_2O_2 into harmless water and oxygen. The neuronal cytoplasmic isoform of the first enzyme group is superoxide dismutase 1 (SOD1) [13]. In the second enzyme group, there are the peroxiredoxin (Prx) and glutathione peroxidase (GPx) families, as well as catalase localized within peroxisomes. Unlike in SOD1 and catalase, enzymes of the Prx and GPx families require secondary enzymes and cofactors to function at high efficiency [7]. The enzymes of the Prx and GPx families are considered to play important roles in the direct control of the redox system. In general, the redox system regulates versatile control mechanisms in signal transduction and gene expression [35]. In mammalian cells, this redox signal transduction is synchronously linked to important systems such as cellular differentiation, immune response, growth control, apoptosis, and tumor growth [4, 9, 19, 26, 31, 34]. In the mammalian central nervous system (CNS), the members of Prx and GPx families regulating the neuronal cytoplasmic redox system are Prxll and GPxl, which directly control the redox system in neurons [6, 7, 8, 12, 17, 24, 27, 29, 30]. In the in vivo milieu where mutant SOD1 exists, Prxll/GPxl co-aggregates with SOD1 as neuronal Lewy body-like hyaline inclusions (LBHIs): neuronal LBHIs immunohistochemically positive for three proteins of SOD1, Prxll and GPxl are observed in the mutant SOD1-related familial ALS (FALS) patients and transgenic rats expressing human SOD1 with H46R and G93A mutations [24]. Although some motor neurons with SOD1 gene mutation form inclusions that are positive for these three proteins, other SOD1-mutated motor neurons progress to cell death without forming the inclusions.

On the other hand, an essential histopathological feature of ALS is loss of the large anterior horn cells throughout the spinal cord, with the surviving motor neurons of the spinal cord exhibiting shrinkage. Among these residual large anterior horn cells, some appear to be normal. These surviving motor neurons in ALS patients are thought to possess some form of self-preservation mechanism. To gain new insight into the survival mechanism of these residual motor neurons, we focused on the redox system. In the study presented here, we performed immunohistochemical analyses of the spinal cord, not only from FALS patients with SOD1 gene mutations and SOD1-mutated ALS animal models, but also from patients with sporadic ALS (SALS), and analyzed the expression of Prxll/GPxl (redox system) in the residual motor neurons.

Materials and methods

Autopsy specimens

Histochemical and immunohistochemical studies were performed on archival, buffered 10% formalin-fixed, paraffin-embedded spinal cord tissues obtained at autopsy from 40 SALS patients and 5 FALS patients, who were members of two different families. The main clinical characteristics of the SALS patients are summarized in Fig. 2. The clinicopathological characteristics of the FALS patients are summarized in Table 1 and have been reported previously [20, 21, 25, 28, 33, 36, 38]. SOD1 analysis revealed that the members of the Japanese Oki family had a two-base pair deletion at codon 126 (frameshift 126 mutation) [20] and that the members of the American C family had an Ala to Val substitution at codon 4 (A4V) [36]. As controls for human samples, we examined autopsy specimens of the spinal cord from 20 neurologically and neuropatho-

Table 1 Characteristics of five FALS cases (*FALS* familial amyotrophic lateral sclerosis, *SOD* superoxide dismutase, *LBHI* Lewy body-like hyaline inclusion, *2-bp* two-base pair, *PCI* posterior column involvement type, + detected, *ND* not determined, *As* asphyxia, *IH* intraperitoneal hemorrhage, *RD* respiratory distress, *Pn* pneumonia)

Case	Age	Sex	Cause of death	FALS duration	SOD1 mutation	FALS subtype	Neuronal LBHI
Japanese Oki family							
1	46	F	As	18 months	2-bp deletion (126)	PCI	+
2	65	M	IH	11 years	2-bp deletion (126)	PCI and degeneration of other systems	+
American C family							
3	39	M	RD	7 months	A4V	PCI	+
4	46	M	Pn	8 months	A4V	PCI	+
5	66	M	Pn	1 year	ND	PCI	+

logically normal individuals (11 males, 9 females; aged 37–75 years).

Animal models

Histochemical and immunohistochemical studies were also carried out on specimens from ALS animal models: transgenic rats and mice carrying the overexpressed human mutant SOD1 genes. The H46R rats used in this study were a transgenic line (H46R-4) in which the level of human SOD1 with the H46R mutation was 6 times the level of endogenous rat SOD1 [32]. The G93A rats were a transgenic line (G93A-39) in which the level of human SOD1 with the G93A mutation was 2.5 times the level of endogenous rat SOD1 [32]. The G93A mice used in this study represented two lines of transgenic mice carrying the overexpressed human G93A mutant SOD1 gene: high copy G93A mice [B6SJL-TgN(SOD1-G93A)1Gur, JR2726; G1H-G93A] and low copy G93A mice [B6SJL-TgN(SOD1-G93A)1Gur^{dl}, JR2300; G1L-G93A] (Jackson Laboratory, Bar Harbor, ME). The H46R rats were killed at 110 ($n=1$), 135 ($n=1$), 160 ($n=1$), 170 ($n=1$), and over 180 ($n=3$) days after birth. The G93A rats were killed at 70 ($n=1$), 90 ($n=1$), 110 ($n=1$), 130 ($n=1$), 150 ($n=1$), and over 180 ($n=3$) days after birth. The detailed clinical signs and pathological characteristics of the H46R and G93A rats have been demonstrated previously [32]. As rat controls, we investigated the spinal cord specimens of each of eight age-matched littermates of the H46R and G93A rats. The G1H-G93A mice were examined at 90 ($n=2$), 100 ($n=2$), 110 ($n=3$), and 120 ($n=3$) days of age. The G1L-G93A mice were examined at 90 ($n=1$), 100 ($n=1$), 120 ($n=1$), 150 ($n=1$), 180 ($n=1$), 190 ($n=1$), 215 ($n=1$), 230 ($n=1$), and over 250 ($n=2$) days of age. As mouse controls, we also examined the spinal cord specimens of each of ten age-matched littermates of the G1H-G93A and G1L-G93A mice. Rats and mice were anesthetized with sodium pentobarbital (0.1 ml/100 g body weight). After perfusion of the animals via the aorta with physiological saline at 37°C, they were fixed by perfusion with 4% paraformaldehyde in 0.1 M cacodylate buffer (pH 7.3). The spinal cords were removed and then postfixed in the same solution. This study was approved by the Institutional Animal Care and Use Committee of Tottori University (Permission no. 03-S-18).

Histochemistry and immunohistochemistry

After fixation, the specimens were embedded in paraffin, cut into 6-μm-thick sections and examined by light microscopy. Spinal cord sections were stained by the following histochemical methods: hematoxylin and eosin (HE), Klüver-Barrera, Holzer, phosphotungstic acid-hematoxylin, periodic acid-Schiff, alcian blue, Masson's trichrome, Mallory azan, and Gallyas-Braak stains.

Rat PrxII, which contained a 6-His-tagged sequence at the N-terminal region, was overexpressed using *Escherichia coli* strain BL21 (DE3) cells harboring the expression plasmid pET30a (Novagen, Darmstadt, Germany) -PrxII, according to the modified method by Hirotsu et al. [15]. The His-tagged PrxII induced with 0.1 mM isopropyl-β-D-thiogalactoside (IPTG) was purified by a Ni^{2+}-nitrilotriacetate column (Qiagen, Hilden, Germany) and then digested with enterokinase. Finally, the purified PrxII was passed through an Erapture Agarose column for removal of enterokinase (Novagen). The PrxII gene was prepared from a rat liver cDNA library (Takara Biomedicals, Otsu, Japan) by PCR using the primers, 5'-TTCCATGGCCTCCGG-CAACGCGCACAT-3' and 5'-TTGGATCCATCTCA-GTTGTGTTTGGAG-3'. Utilizing this purified recombinant rat Prxll protein (amino acids 1–198), we produced a rabbit polyclonal antibody against rat PrxII according to the method previously described by Kato et al. [24].

Representative paraffin sections were used for immunohistochemical assays. The following primary antibodies were used: a rabbit polyclonal antibody against rat Prxll (amino acids 1–198) [diluted 1:2,000 in 1% bovine serum albumin-containing phosphate-buffered saline (BSA-PBS), pH 7.4]; an affinity-purified rabbit antibody against a synthetic peptide corresponding to the C-terminal region of Prxll (amino acids 184–198; this amino acid sequence is homologous with those of the C-terminal regions of the human, rat or mouse Prxll.) (concentration: 1 μg/ml) [24]; a polyclonal antibody to GPxl [diluted 1:2,000 in 1% BSA-PBS, pH 7.4] [3]; a polyclonal antibody to human SOD1 (diluted 1:10,000 in 1% BSA-PBS, pH 7.4) [2]; and a monoclonal antibody to human SOD1 (concentration: 3 μg/ml; MBL, Nagoya, Japan). Sections were deparaffinized, and endogenous peroxidase activity was quenched by incubation for 30 min with 0.3% H_2O_2. The sections were then washed in PBS. Normal sera homologous with the secondary antibodies were used as a blocking reagent. Tissue sections were incubated with the primary antibodies for 18 h at 4°C. PBS-exposed sections served as controls. As a further control, some sections were incubated with the polyclonal antibody against rat Prxll that had been preabsorbed with an excess amount of the recombinant rat Prxll protein. Bound antibodies were visualized by the avidin-biotin-immunoperoxidase complex (ABC) method using the appropriate Vectastain ABC kits (Vector Laboratories, Burlingame, CA) and 3,3'-diaminobenzidine tetrahydrochloride (DAB; Dako, Glostrup, Denmark) as chromogen.

Western blot analysis

This analysis was carried out on three fresh autopsy specimens from spinal cord cervical segments obtained from two SALS cases [2.5 years after onset (case 19 in Fig. 2: age 63 years) and 11 years 5 months after onset

(case 40 in Fig. 2: age 51 years)] and one normal individual (age 68 years). In brief, specimens were homogenized in Laemmli sample buffer (Bio-Rad, Hercules, CA) containing 2% sodium dodecyl sulfate (SDS), 25% glycerol, 10% 2-mercaptoethanol, 0.01% bromophenol blue, and 62.5 mM TRIS-HCl (pH 6.8). The samples were heated at 100°C for 5 min. Soluble protein extracts (20 μg) from the samples were separated on SDS-polyacrylamide gels (4–20% gradient, Bio-Rad) and transferred by electroblotting to Immobilon PVDF (Millipore, Bedford, MA). After blocking with 5% nonfat milk for 30 min at room temperature, the blots were incubated overnight at 4°C with the antibodies against PrxII and GPxI. Binding to PrxII and GPxI was visualized with the Vectastain ABC Kit and DAB. Appropriate molecular weight markers (Bio-Rad) were included in each run.

Results

Histopathology

An important histopathological finding in the spinal cord in SALS was loss of motor neurons throughout the

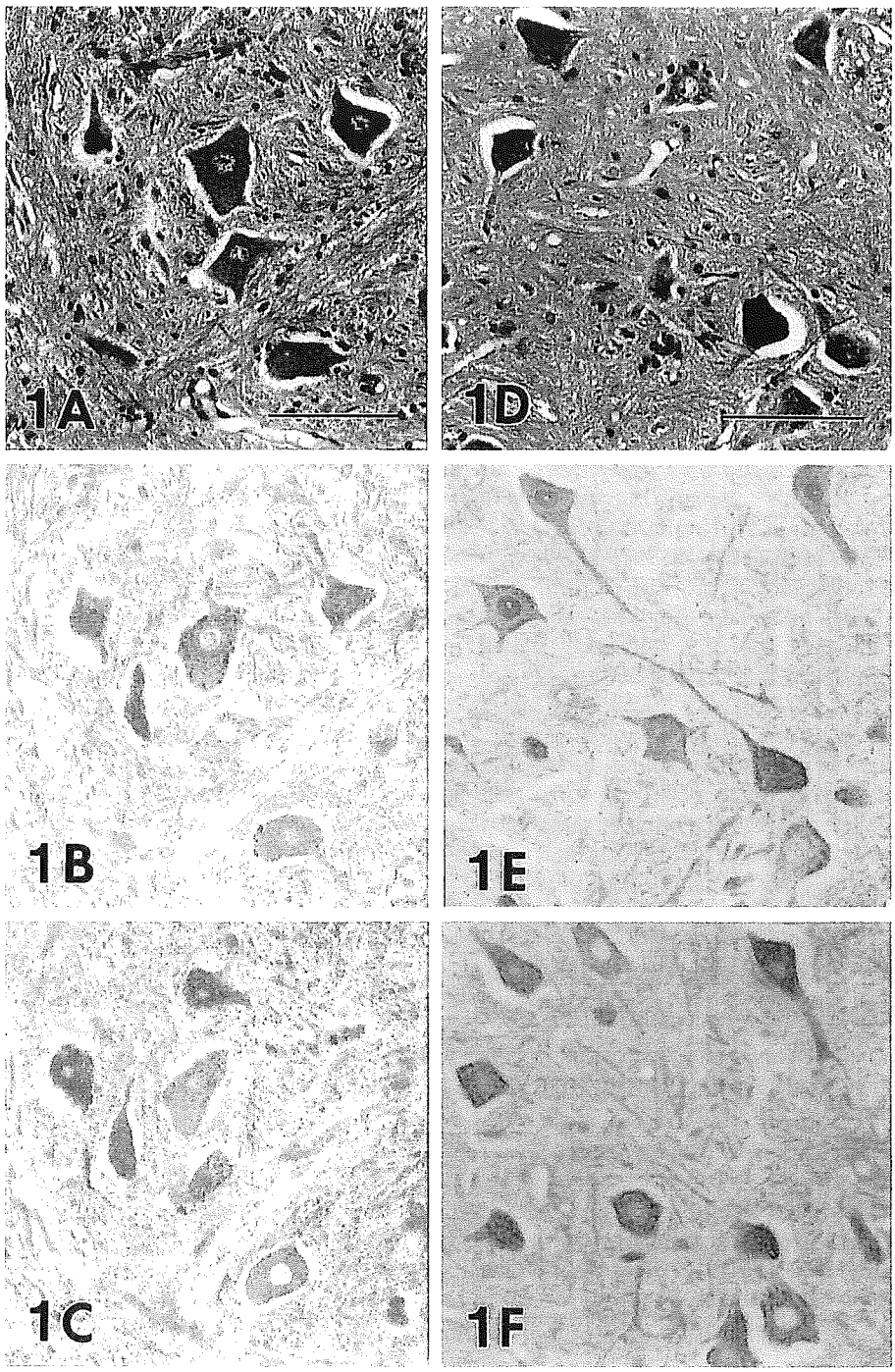

Fig. 1 Detection of PrxII and GPxI in serial sections of the normal anterior horn cells of the spinal cord in humans (**A–C**) and rats (**D–F**). **A, D** HE staining. **B, E** Immunoreactive for PrxII: immunostaining with the antibody against synthetic peptide corresponding to the C-terminal region of PrxII (**B**) and immunostaining with the antibody to rat PrxII (**E**). Immunoreactivity is identified in most of the anterior horn cells. **C, F** Immunostaining for GPxI. Almost all of the anterior horn cells in the spinal cord coexpress both PrxII (**B, E**) and GPxI (**C, F**) in comparison with HE-stained serial sections (**A, D**), although their staining intensities in neurons vary. **B, C, E, F** No counterstaining. (*HE* hematoxylin and eosin, *PrxII* peroxiredoxin-II, *GPxI* glutathione peroxidase-I). *Bars* **A** (also for **B, C**), **D** (also for **E, F**) 100 μm

course of the disease. In the specimens we examined, neuronal loss was most easily recognized in the cervical and lumbar enlargements. The surviving motor neurons showed shrinkage, and lipofuscin granule-filled neurons stood out. Among the residual motor neurons, some appeared to be normal. Bunina bodies were observed in the residual motor neurons. The number of motor neurons decreased with SALS disease progression. Reactive astrocytosis and gliosis were also observed in the affected areas. In the affected antero-lateral columns that were most pronounced in the crossed and uncrossed corticospinal tracts, there was a loss of large myelinated fibers in association with variable degrees of astrocytic gliosis. Fiber destruction was associated with the appearance of lipid-laden macrophages. Analysis of the essential changes in the five cases of SOD1-mutated FALS revealed a subtype of FALS with posterior column involvement (PCI). This subtype is characterized by degeneration of the middle root zones of the posterior column, Clarke nuclei, and the posterior spinocerebellar tracts, in addition to spinal cord motor neuron lesions. A patient who had survived for a long period, with a clinical course of 11 years (case 2 in Table 1), showed multi-system degeneration in addition to the features of FALS with PCI. Neuronal LBHIs were present in all five FALS cases with SOD1 gene mutations. The spinal cords of normal human individuals did not exhibit any distinct histopathological alterations.

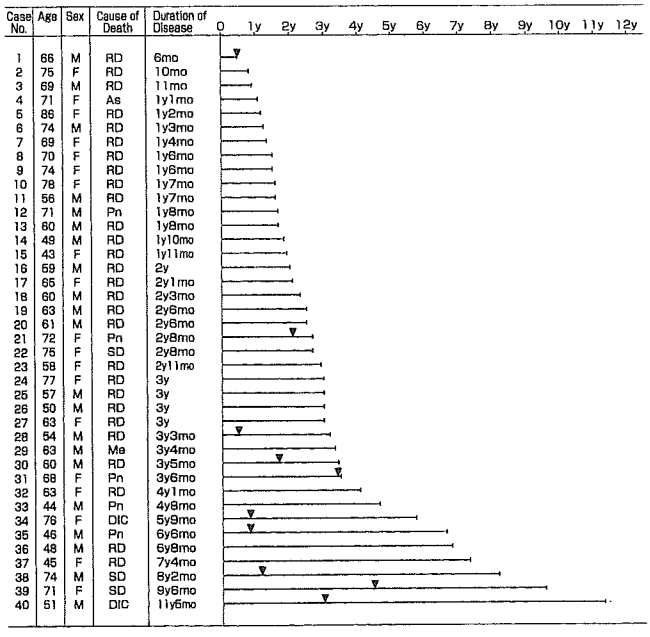

Fig. 2 Characteristics of 40 SALS cases, including patient's age, sex, cause of death, and duration of disease. The *horizontal lines* each show the duration of disease. *Arrowheads* indicate the time point at which the patients were placed on respirators (*ALS* amyotrophic lateral sclerosis, *SALS* sporadic ALS, *RD* respiratory distress, *As* asphyxia, *Pn* pneumonia, *SD* sudden death, *Me* melena, *DIC* disseminated intravascular coagulation, *y* years, *mo* months)

The clinical courses and histopathological findings of H46R and G93A transgenic rats have been reported previously by Nagai et al. [32]. As expected, the H46R rats developed motor deficits at approximately 145 days of age, and G93A rats showed the clinical signs at around 125 days of age. When we focused on the anterior horn cells, the number of the anterior horn cells of the H46R rat at 110 days of age was not significantly decreased as compared with that of the age-matched littermate. There were slightly decreased numbers of anterior horn cells with inclusions in the H46R rat at 135 days of age. At 160, 170 and over 180 days of age, the number of the anterior horn cells in the H46R rats was decreased markedly, and many inclusions including neuronal LBHIs were observed as inclusion pathology. For G93A rats, the number of the anterior horn cells at 70, 90 and 110 days of age was almost the same as that of their age-matched littermates, although at 90 and 110 days of age these rats showed vacuolation pathology including neuropil vacuoles. In G93A rats at 130, 150 and over 180 days of age, there was marked loss of the anterior horn cells, with both inclusion and vacuolation pathologies being involved. In the transgenic mice from the Jackson Laboratory, the clinical onset of the G1H-G93A mice was, as expected, about 100 days after birth, and that of G1L-G93A mice was approximately 185 days after birth. The number of the anterior horn cells of the G1H-G93A mice examined at 90 days after birth was not significantly decreased as compared with that of their age-matched littermates, whereas neuropil vacuolation was observed. The number of anterior horn cells of the G1H-G93A mice at 100 days of age was slightly decreased, and they had abundant vacuoles and a few inclusions. The G1H-G93A mice examined at 110 and 120 days of age revealed severe loss of the anterior horn cells and both inclusion and vacuolation pathologies. In the G1L-G93A mice examined at 90, 100, 120, 150 and 180 days after birth, the number of the anterior horn cells was not significantly changed compared to that of their age-matched littermates, although the G1L-G93A mice at 90, 100, 120, 150 and 180 days of age showed vacuolation pathology and, at 180 days of age, a few inclusions. In G1L-G93A mice at 190, 215, 230 and over 250 days of age, there were significant losses of anterior horn cells, with both inclusion and vacuolation pathologies being present. The spinal cords of the littermates of these animal models did not exhibit any distinct histopathological changes.

Immunohistochemistry

In the present study, we produced a rabbit polyclonal antibody against rat Prxll (amino acids 1–198), in addition to the affinity-purified rabbit antibody against a synthetic peptide corresponding to the C-terminal region of Prxll previously reported by Kato et al. [24]. This newly produced rabbit polyclonal antibody against rat Prxll was successfully applied to stain paraffin sections

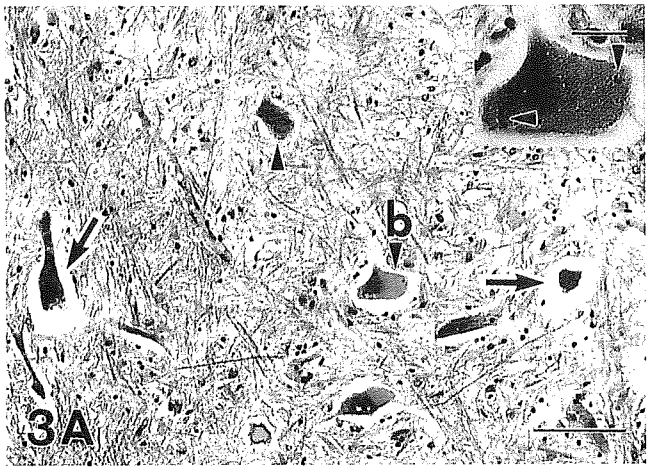

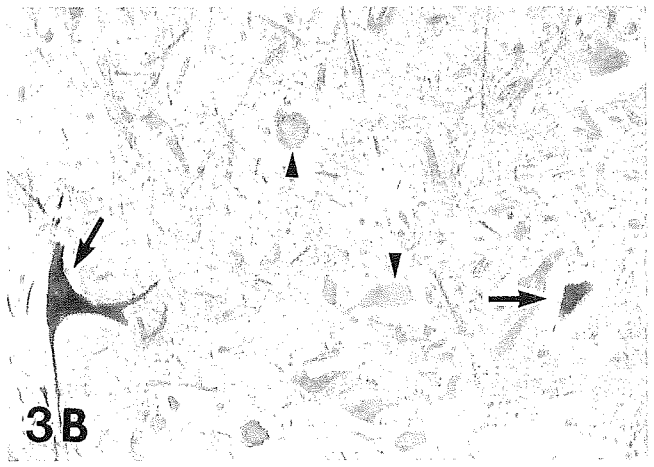

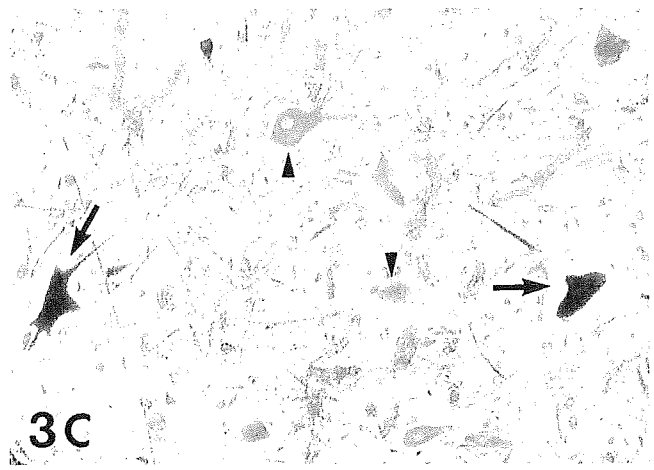

◀

Fig. 3 Serial sections of the spinal anterior horn cells in a patient with SALS after a clinical course of 2.5 years (case 19 in Fig. 2). **A** Light microscopic preparation stained with HE. *Top right inset* shows the higher magnification of a neuron (indicated by *arrowhead* with **b** in **A**), in which Bunina bodies (*arrowheads* in *top right inset*) are observed. **B** PrxII immunoreactivity of the section consecutive to that shown in **A**. **C** GPxI immunoreactivity of the section consecutive to that shown in **B**. Residual neurons overexpressing both PrxII and GPxI are evident (*arrows*). The staining pattern is diffuse in the cytoplasm and dendrites. Other neurons are either faintly stained by both antibodies, or unstained (*arrowheads*). Observation of only the HE-stained section in **A** reveals no difference between the neurons overexpressing PrxII/GPxI and those almost negative for PrxII/GPxI. No correlation is demonstrated between PrxII/GPxI expression and the presence of Bunina bodies. **B**, **C** No counterstaining. *Bar* **A** (also for **B**, **C**) 100 μm, *top right inset* in **A** 20 μm

from rats (Fig. 1E). Additionally, we were able to use this rabbit polyclonal antibody against rat Prxll to stain paraffin sections from humans and mice. Both anti-Prxll antibodies had the same ability to immunostain paraffin sections from humans, rats and mice, as well as in immunoblotting of tissue homogenate of the human spinal cord. When control and representative paraffin sections were incubated with PBS alone (i.e., no primary antibody), no staining was detected. Incubation of sections with anti-rat Prxll antibody that had been pretreated with an excess amount of the recombinant rat Prxll protein (amino acids 1–198) produced no staining in any of the sections.

As expected [24], almost all of the normal anterior horn cells in the spinal cords of humans, rats and mice coexpressed both Prxll and GPxl (Fig. 1), although their staining intensities in positively stained neurons varied. With respect to the intracellular localization of Prxll using the two anti-Prxll antibodies, immunostaining of the neuronal cytoplasm and proximal dendrites was specifically observed (Fig. 1B, E). In addition, the nuclei of some neurons were immunostained, albeit the staining intensity varied (Fig. 1E). GPxl immunostaining showed a cytoplasmic staining pattern, with the cell bodies and proximal dendrites being essentially identified (Fig. 1C, F), but no intranuclear staining was observed (Fig. 1C, F).

In SALS patients, some residual neurons expressed both Prxll and GPxl strongly within about 3 years after disease onset (cases 1–27 in Fig. 2). Other neurons were either faintly stained by both antibodies or unstained. Around 2–3 years after disease onset in SALS patients (cases 16–27 in Fig. 2), the intensity of Prxll and GPxl immunoreactivities peaked in some residual neurons that were positive for both proteins (Fig. 3). In SALS patients with a clinical course of over 3 years (cases 28–40 in Fig. 2), the number of residual neurons decreased strikingly, and respiratory assistance became essential for most patients. The residual neurons intensely expressing both Prxll and GPxl decreased with disease progression, while the number of residual neurons negative for both proteins increased dramatically (Fig. 4). At 11 years 5 months after disease onset (case 40 in Fig. 2), most of the neurons were atrophic and immunonegative for both Prxll and GPxl. However, even in this long-surviving patient, a few residual neurons expressing both Prxll and GPxl were observed (Fig. 5). Thus, residual motor neurons positive for both Prxll and GPxl were always evident throughout the disease course in every SALS patient, although after approximately 3 years of disease their number decreased dramatically. Observation of only the HE-stained sections revealed no

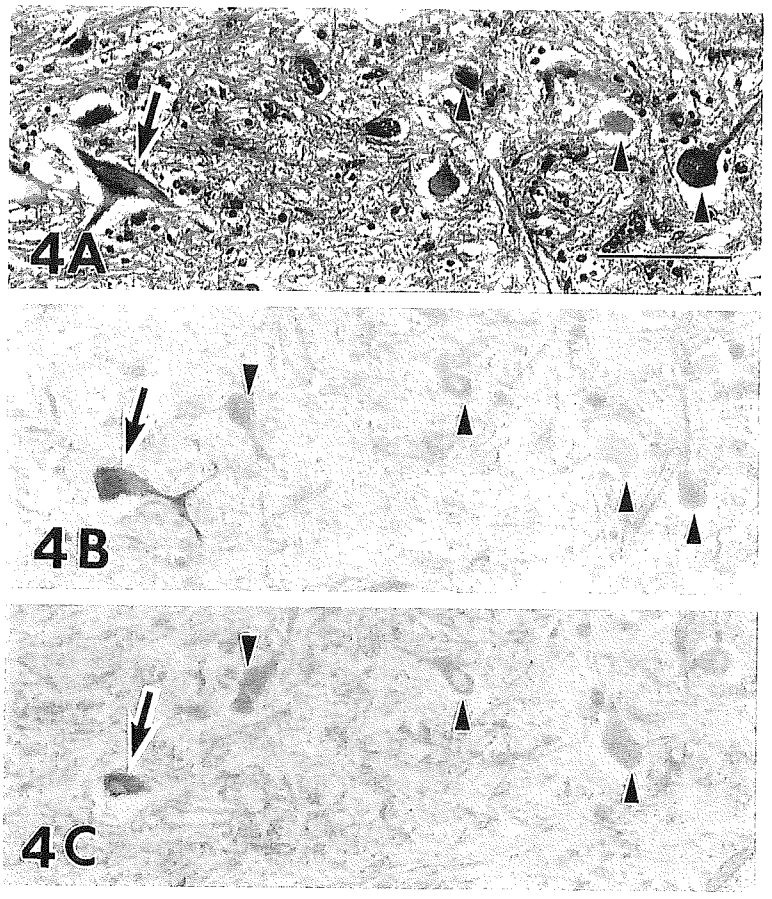

Fig. 4 Serial sections of the spinal anterior horn cells in a patient with SALS after a clinical course of 4 years 8 months (case 33). **A** In the HE preparation, residual motor neurons appear to be atrophic. There is no distinction among these atrophic neurons when observed in the HE preparation alone. **B** Immunostaining for Prxll. The number of residual neurons overexpressing Prxll (*arrow*) is reduced in comparison with that in the SALS patient after a clinical course of 2.5 years (Fig. 3). The number of Prxll-negative neurons is increased (*arrowheads*). **C** Immunostaining for GPxl. Similarly to the Prxll immunostaining, the number of GPxl-overexpressing neurons is diminished (*arrow*). In contrast, the number of GPxl-immunonegative neurons is increased (*arrowheads*). **B, C** No counterstaining. *Bar* **A** (also for **B, C**) 100 μm

difference between the neurons positive for Prxll and GPxl and those negative for both proteins (Figs. 3, 4, 5).

In the five FALS patients with SOD1 mutations, as reported previously [24], neuronal LBHIs in the anterior horn cells showed co-aggregation of Prxll/GPxl with SOD1. Although some SOD1-mutated anterior horn cells in these patients formed neuronal LBHIs, others did not. When we focused on these residual anterior horn cells without inclusions, the stainability and intensity of Prxll and GPxl staining in the residual cells without inclusions in the five FALS patients with SOD1 gene mutations were identical to those of the SALS patients. The numbers of residual anterior horn cells in one member of the Japanese Oki family (case 1, frame-shift 126 mutation in SOD1 gene) and three members of the American C family (cases 3–5, A4V substitution in the SOD1 gene), observed within 2 years of the disease onset, were similar, although the loss of the anterior horn cells in the FALS patients was generally more severe in contrast to that seen in the SALS patients with the same disease duration. As in the SALS patients within about 3 years of disease onset, some of the residual anterior horn cells with no LBHIs overexpressed Prxll/GPxl in the four short-term-surviving FALS patients from the two different families and divergent SOD1 gene mutations. In a long-term surviving patient (case 2) with a clinical course of over 10 years, there were a few residual neurons, and most were immunonegative for Prxll/GPxl. However, rare residual neurons expressing Prxll/GPxl were still evident. The findings for the long-term-surviving FALS patient with SOD1 mutation were the same as those of the long-term-surviving SALS patients.

In the ALS animal models with human mutant SOD1, the inclusions exhibited co-aggregation of Prxll/GPxl with SOD1 as reported previously [24]. Noticeably, the Prxll/GPxl-immunoreactive findings in the rat (H46R and G93A rats) and mouse (G1H-G93A and G1L-G93A mice) models were essentially the same throughout the disease course for each ALS animal model. In the preclinical stage, the Prxll/GPxl immunostainability and immunointensity of the anterior horn cells were identical to those in the anterior horn cells of the normal littermates. Although the number of the anterior horn cells in the ALS animal models was decreased after the clinical onset of disease, some of these residual anterior horn cells showed overexpression of Prxll/GPxl, i.e., up-regulation of the redox system. In particular, this redox system up-regulation in the residual motor neurons was prominent at 160 days of age in H46R rats (Fig. 6A, B), at 150 days of age in G93A rats, at 110 days of age in G1H-G93A mice (Fig. 7) and at 215 days of age in G1L-G93A mice. At the end stage of disease in the four different ALS animal models,

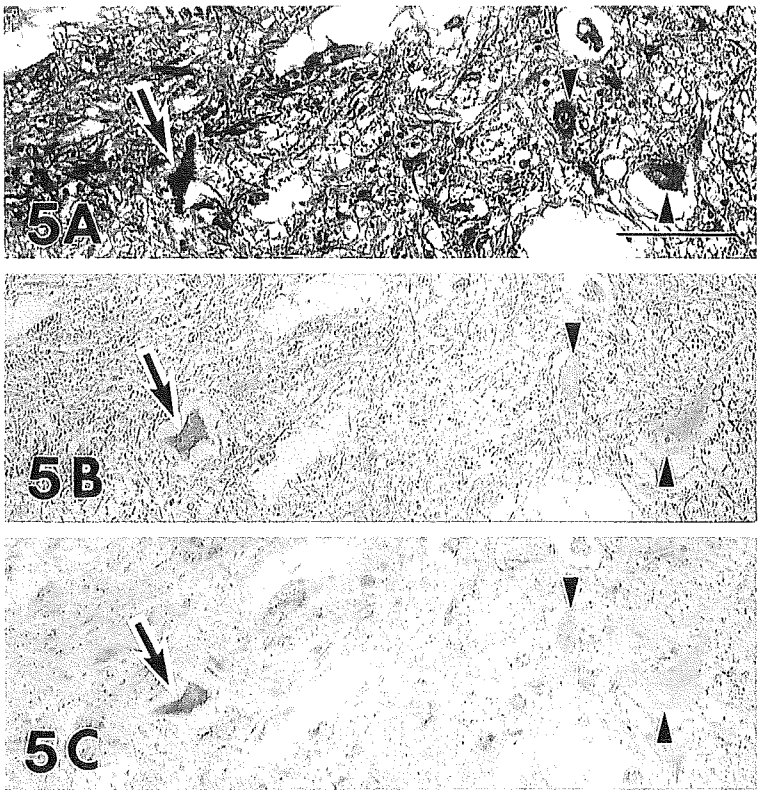

Fig. 5 Serial sections of the spinal anterior horn cells in a patient with SALS after a clinical course of 11 years 5 months (case 40). **A** Light microscopic preparation stained with HE. Small and atrophic motor neurons are seen. **B** Prxll immunoreactivity of the section consecutive to that shown in **A**. Although the residual neuron (*arrow*) appears to be atrophic in the HE preparation, this residual neuron expresses Prxll. **C** GPxl immunoreactivity of the section consecutive to that shown in **B**. The residual neuron that appears to be atrophic in the HE preparation is stained by the anti-GPxl antibody (*arrow*). Although there is no neuron overexpressing Prxll/GPxl, a neuron expressing Prxll/GPxl can be observed (*arrow*). By marked contrast, the number of neurons negative for Prxll/GPxl is increased (*arrowheads*). Observation of the HE-stained section in **A** shows no difference between the atrophic neuron positive for Prxll/GPxl (*arrow*) and the atrophic neurons negative for both proteins (*arrowheads*). **B**, **C** No counterstaining. *Bar* **A** (also for **B**, **C**) 100 μm

however, almost all of the residual motor neurons were negative for Prxll/GPxl, in marked contrast to the inclusions positive for PrxII/GPxI (Fig. 6C, D). As seen for the human specimens, no difference between the neurons positive for Prxll/GPxl and those negative for both proteins were observed the HE-stained sections for these animal models (Fig. 7).

Western blot analysis

When the tissue homogenate of each fresh cervical segment of the human spinal cord was examined by immunoblotting for Prxll, a single band corresponding to approximately 23 kDa was observed, i.e., with the same mobility as human Prxll (Fig. 8A). Immunoblotting showed that the intensity of Prxll immunoreactivity in the SALS patient with a clinical course of 2.5 years (case 19 in Fig. 2) appeared to be almost identical to that in a normal subject. In the SALS patient with a clinical course of 11 years 5 months (case 40 in Fig. 2), Prxll expression was less than that in the normal subject. This observation supported the results of Prxll immunohistochemistry. Immunoblotting for GPxl revealed a single band corresponding to about 22 kDa in two SALS cases and a normal subject (Fig. 8B). This molecular mass was compatible with that of human GPxl. In the SALS case at 2.5 years after disease onset (case 19 in Fig. 2), GPxl was expressed with almost the same intensity as that in the normal subject. However, the level of GPxl expression in the SALS case at 11 years 5 months after onset (case 40 in Fig. 2) decreased below that in the normal subject. This finding reflected the GPxl immunohistochemistry results.

Discussion

Prxll is a novel organ-specific anti-oxidative enzyme that is mainly expressed in mammalian brain [24, 29]. It is a member of the Prx family, the members of which directly regulate the redox system [6, 7, 8, 17, 29]. Prxll is a homodimeric protein composed of two subunits, each with a molecular mass of approximately 23 kDa [15, 16]. Like Prxll, GPxl, one of the major cytosolic isoforms of the GPxl family, also directly controls the redox system [12, 27, 30]. GPxl is a homotetramer consisting of approximately 22-kDa subunits [3]. This is consistent with the results of Western blot analyses, where use of

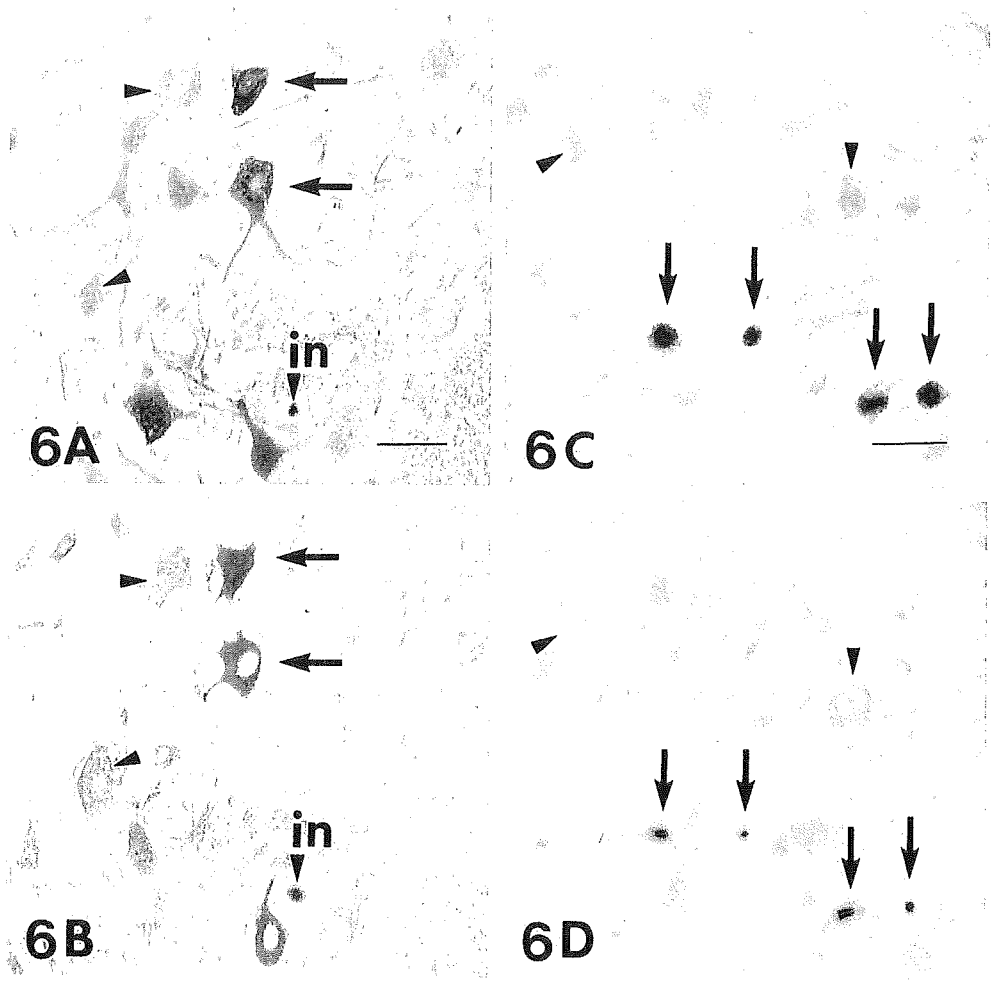

Fig. 6 Expression of Prxll and GPxl detected by immunohistochemistry in the spinal anterior horn in the transgenic rats expressing human SOD1 with an H46R mutation. **A, B** Serial sections of spinal anterior horn cells at 160 days of age in H46R rat immunostained with antibodies against Prxll (**A**) and GPxl (**B**). Residual neurons overexpressing Prxll/GPxl, i.e., showing redox system up-regulation, are observed (*arrows*). An inclusion (*arrowhead* with *in*) in the neuropil is intensely positive for Prxll/GPxl. The other neurons are either faintly stained by both antibodies, or unstained (*arrowheads*). **C, D** Serial sections of spinal anterior horn cells at over 180 days of age in H46R rat immunostained with antibodies against Prxll (**C**) and GPxl (**D**). Round and sausage-like LBHIs are strongly positive for Prxll/GPxl (*arrows*). By marked contrast, the number of neurons negative for Prxll/GPxl is increased (*arrowheads*). **A—D** No counterstaining (*SOD* superoxide dismutase, *LBHI* Lewy body-like hyaline inclusion). *Bar* **A** (also for **B**) 50 μm, **C** (also for **D**) 30 μm

the normal human tissue homogenate yielded a single band of approximately 23 kDa with the two anti-Prxll antibodies and a single band of about 22 kDa with the anti-GPxl antibody.

As expected [24], Prxll/GPxl immunoreactivity in anterior horns of the normal spinal cords of humans, rats and mice was primarily identified in the neurons: cytoplasmic staining was observed in almost all of the anterior horn cells. Intranuclear localization in some neurons was also observed with Prxll immunostaining using the two anti-Prxll antibodies, as previously reported [24]. Considering that endogenous Prxll and GPxl within the neuronal cytoplasm are regulators of the redox system, our finding that almost all of the normal spinal motor neurons coexpressed Prxll/GPxl confirms that these motor neurons maintain themselves utilizing the intracellular Prxll/GPxl system, that is, the redox system.

Corroborating previous findings [24], neuronal LBHIs positive for SOD1, Prxll, and GPxl were observed in both the SOD1-mutated FALS patients and the four transgenic ALS animal models expressing human mutant SOD1. A breakdown of the redox system was seen in the SOD1-mutated motor neurons containing inclusions. It is possible that the intra-inclusional co-aggregation of Prxll/GPxl with SOD1, or the sequestration of Prxll/GPxl with SOD1 into the inclusions causes the intracytoplasmic reduction of Prxll/GPxl, thereby reducing the availability of the redox system [24]. Although inclusions were seen in some motor neurons with the SOD1 gene mutation, other SOD1-mutated motor neurons progressed to the cell death without forming the inclusions.

An interesting feature was the presence of certain residual motor neurons coexpressing Prxll/GPxl throughout the ALS disease course in SALS patients and among SOD1-mutated motor neurons without inclusions. A particularly striking finding was that motor neurons overexpressing Prxll/GPxl, i.e., with redox system up-regulation, were commonly evident during the clinical courses in the divergent disease subtypes: SALS patients, SOD1-mutated FALS patients, and ALS animal models expressing human mutant SOD1.

For the SALS patients, although the number of the residual SALS motor neurons decreased with the progression of the clinical disease, some motor neurons overexpressing Prxll/GPxl were present usually up to approximately 3 years after the onset, particularly in the

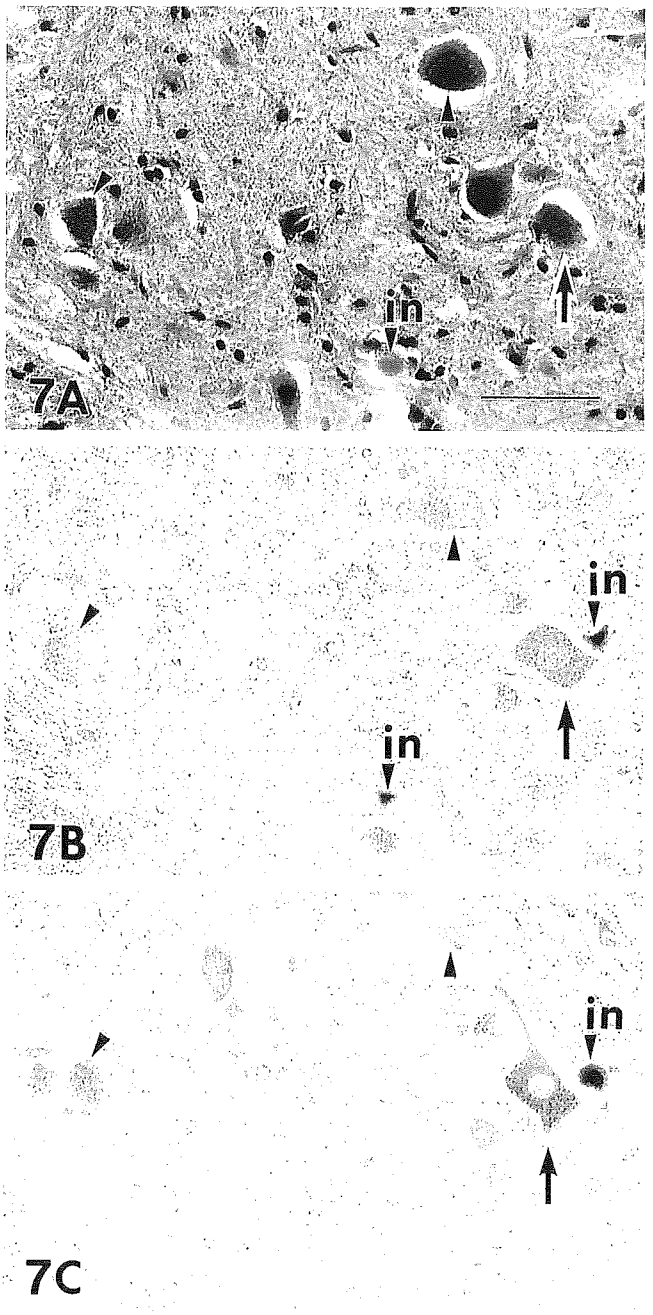

Fig. 7 Expression of Prxll and GPxl detected by immunohistochemistry in the spinal anterior horn in a G1H-G93A transgenic mouse carrying the highly overexpressed human G93A mutant SOD1 gene at 110 days of age. **A** Light microscopic preparation stained with HE. A round LBHI in the neuropil can be seen (*arrowhead* with *in*). **B** Prxll immunoreactivity of the section consecutive to that shown in **A**. **C** GPxl immunoreactivity of the section consecutive to that shown in **B**. Like in human ALS (Figs. 3, 4) and H46R rat (Fig. 6), a residual neuron overexpressing Prxll/GPxl, i.e., showing redox system up-regulation, can be observed (*arrow*). The other neurons are either faintly stained by both antibodies, or unstained (*arrowheads*), which indicates the breakdown of redox system. Round and sausage-like LBHIs in the neuropil are strongly positive for Prxll/GPxl (*arrowhead* with *in*). Observation of the HE-stained section in **A** reveals no difference between the neuron showing the redox system up-regulation (*arrow*) and the neurons exhibiting the redox system breakdown (*arrowheads*). **B, C** No counterstaining. *Bar* **A** (also for **B**, **C**) 50 μm

patients with no respiratory assistance. Thereafter, the number of these overexpressing motor neurons decreased dramatically as disease progressed. The immunohistochemical features are consistent with the Western blot findings that the levels of the Prxll/GPxl in the SALS patient after a clinical course of 2.5 years were almost the same levels as in normal cases in spite of loss of the motor neurons, whereas the levels decreased in the SALS patient after a clinical course of 11 years 5 months.

In the SOD1-mutated FALS patients, as in SALS patients, certain residual motor neurons without LBHIs also overexpressed Prxll/GPxl in the four short-term-surviving patients within 18 months after onset. In the ALS animal models, as in the human diseases, some residual motor neurons showed overexpression of Prxll/GPxl at 160 days of age in H46R rats, at 150 days of age in G93A rats, at 110 days of age in G1H-G93A mice and at 215 days of age in G1L-G93A mice. The presence of this common Prxll/GPxl-overexpression mechanism during the clinical course of ALS suggests that the redox system up-regulation represents one of the endogenous mechanisms that are activated by the ALS stress. At the terminal stage of ALS, however, disruption of this mechanism was observed. Although some residual ALS neurons coexpressed both proteins, while many others were negative, there was no apparent difference among these neurons on HE preparations.

In general, the redox system is one of the most crucial life supporting systems in living cells, serving as an antioxidant enzyme defense system that is synchronously linked to important physiological functions such as cellular differentiation, immune response, growth control, apoptosis, and tumor growth [4, 9, 19, 26, 31,

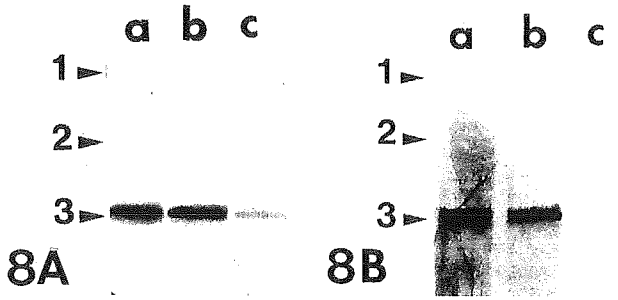

Fig. 8 Western blot analyses using the antibodies against Prxll (**A**) and GPxl (**B**). A 20-μg sample of the soluble protein extract from each sample was applied to each lane. Molecular mass markers: *1* ovalbumin (45 kDa); *2* carbonic anhydrase (31 kDa); *3* trypsin inhibitor (21.5 kDa). **A** *Lane a*: Normal control, *lane b*: an SALS patient with a clinical course of 2.5 years (case 19). *lane c*: an SALS patient with a clinical course of 11 years 5 months (case 40). A single band at approximately 23 kDa is observed in all samples. The intensity of Prxll immunoreactivity in *lane b* (ALS case 19) appears to be almost identical to that in *lane a* (normal). By contrast, Prxll expression in *lane c* (ALS case 40) appears to be lower than that in *lane a* (normal). **B** A single band of about 22 kDa is detected in each sample. Expression of GPxl in *lane b* (ALS case 19) shows almost the same intensity as that in *lane a* (normal). However, the level of GPxl expression in *lane c* (ALS case 40) is decreased below that seen in *lane a* (normal)

34]. Although we cannot exclude the possibility that the cells die as a result of redox stress itself, the residual ALS neurons expressing redox system up-regulation are thought to maintain their viability by protecting themselves from potentially destructive ROSs and by controlling the intraneuronal redox system [1, 5, 10, 14, 34, 39]. A similar up-regulation mechanism for hepatocyte growth factor (HGF, a novel neurotrophic factor) and its receptor (c-Met) also occurs in the SALS and SOD1-mutated FALS patients [22]. Considering that in the animal experiment, overexpression of HGF attenuates motor neuron death and prolongs the life span of G1L-G93A mice [37], motor neurons showing up-regulation of the HGF/c-Met cell-survival system, which is normally present in neurons, are thought to show enhanced cell survival in the presence of ALS stress in humans [22]. Although we cannot readily compare the neurotrophic factor with the redox system, our finding leads us to the conclusion that the residual ALS neurons showing redox system up-regulation would be less susceptible to ALS stress and can protect themselves from ALS neuronal death. Taken together with the fact that Prxll functions not only as a member of the redox system but also as a molecular chaperone [18], the residual ALS neurons overexpresing Prxll/GPxl might have developed to possess simultaneously both the enhanced antioxidant enzyme defense mechanism as a highly-evolved redox system, and the amplified sophisticated system for coping with misfolded proteins, such as mutant SOD1 or unknown pathogenetic proteins leading to SALS. Thus, residual ALS neurons overexpressing redox system-related enzymes could protect themselves from ALS stress. However, it is not thought possible for residual ALS neurons under long-term ALS stress to keep on inducing redox system-related enzymes. Therefore, as ALS progresses, the ability of residual neurons to up-regulate the redox system diminishes, and finally they become even unable to maintain the redox system itself. In other words, ALS neurons showing redox system up-regulation might show enhanced cell survival in the presence of ALS stress. In contrast, breakdown of the redox system in ALS motor neurons that are barely viable would result in cell death, and many residual motor neurons that are unable to coexpress Prxll/GPxl would ultimately become moribund.

Our data may lead to the development of a new therapy based on redox system up-regulation for the treatment of ALS, which for over 130 years has had an unknown etiology. It remains to be determined whether this redox system up-regulation is a direct or an indirect effect based on the pathogenesis of ALS itself, or whether this redox system up-regulation plays a primary or a secondary role in attenuating ALS-related neuronal death.

Acknowledgements This study was supported in part by a Research Grant on Measures for Intractable Diseases from the Ministry of Health, Labour and Welfare of Japan (S.K. and Y.I.); a Research Grant (2004) from the Faculty of Medicine, Tottori University (S.K.); a Grant-in-Aid for Scientific Research in Priority Area (T.N.) and a Grant-in-Aid for Scientific Research (Y.A.) from the Ministry of Education Culture, Sports, Science and Technology of Japan.

References

1. Andoh T, Chiueh CC, Chock PB (2003) Cyclic GMP-dependent protein kinase regulates the expression of thioredoxin and thioredoxin peroxidase-1 during hormesis in response to oxidative stress-induced apoptosis. J Biol Chem 278:885–890
2. Asayama K, Burr IM (1984) Joint purification of mangano and cuprozinc superoxide dismutases from a single source: a simplified method. Anal Biochem 136:336–339
3. Asayama K, Yokota S, Dobashi K, Hayashibe H, Kawaoi A, Nakazawa S (1994) Purification and immunoelectron microscopic localization of cellular glutathione peroxidase in rat hepatocytes: quantitative analysis by postembedding method. Histochemistry 102:213–219
4. Berggren MI, Husbeck B, Samulitis B, Baker AF, Gallegos A, Powis G (2001) Thioredoxin peroxidase-1 (peroxiredoxin-1) is increased in thioredoxin-1 transfected cells and results in enhanced protection against apoptosis caused by hydrogen peroxide but not by other agents including dexamethasone, etoposide, and doxorubicin. Arch Biochem Biophys 392:103–109
5. Biteau B, Labarre J, Toledano MB (2003) ATP-dependent reduction of cysteine-sulphinic acid by *S. cerevisiae* sulphiredoxin. Nature 425:980–984
6. Chae HZ, Kim IH, Kim K, Rhee SG (1993) Cloning, sequencing, and mutation of thiol-specific antioxidant gene of *Saccharomyces cerevisiae*. J Biol Chem 268:16815–16821
7. Chae HZ, Chung SJ, Rhee SG (1994) Thioredoxin-dependent peroxide reductase from yeast. J Biol Chem 269:27670–27678
8. Chae HZ, Robison K, Poole LB, Church G, Storz G, Rhee SG (1994) Cloning and sequencing of thiol-specific antioxidant from mammalian brain: alkyl hydroperoxide reductase and thiol-specific antioxidant define a large family of antioxidant enzymes. Proc Natl Acad Sci USA 91:7017–7021
9. Chang TS, Jeong W, Choi SY, Yu S, Kang SW, Rhee SG (2002) Regulation of peroxiredoxin I activity by cdc2-mediated phosphorylation. J Biol Chem 277:25370–25376
10. Chang TS, Jeong W, Woo HA, Lee SM, Park S, Rhee SG (2004) Characterization of mammalian sulfiredoxin and its reactivation of hyperoxidized peroxiredoxin through reduction of cysteine sulfinic acid in the active site to cysteine. J Biol Chem 279:50994–51001
11. Charcot JM, Joffroy A (1869) Deux cas d'atrophie musculaire progressive avec lésions de la substance grise et des faisceaux antéro-latéraux de la moelle épinière. Arch Physiol (Paris) 2:744–760
12. De Haan JB, Bladier C, Griffiths P, Kelner M, O'Shea RD, Cheung NS, Bronson RT, Silvestro MJ, Wild S, Zheng SS, Beart PM, Hertzog PJ, Kola I (1998) Mice with a homozygous null mutation for the most abundant glutathione peroxidase, Gpx1, show increased susceptibility to the oxidative stress-inducing agents paraquat and hydrogen peroxide. J Biol Chem 273:22528–22536
13. Fridovich I (1986) Superoxide dismutases. Adv Enzymol Relat Areas Mol Biol 58:61–97
14. Georgiou G, Masip L (2003) An overoxidation journey with a return ticket. Science 300:592–594
15. Hirotsu S, Abe Y, Nagahara N, Hori H, Nishino T, Okada K, Hakoshima T (1999) Crystallographic characterization of a stress-induced multifunctional protein, rat HBP-23. J Struct Biol 126:80–83
16. Hirotsu S, Abe Y, Okada K, Nagahara N, Hori H, Nishino T, Hakoshima T (1999) Crystal structure of a multifunctional 2-Cys peroxiredoxin heme-binding protein 23 kDa/proliferation-associated gene product. Proc Natl Acad Sci USA 96:12333–12338

17. Ichimiya S, Davis JG, O'Rourke DM, Katsumata M, Greene MI (1997) Murine thioredoxin peroxidase delays neuronal apoptosis and is expressed in areas of the brain most susceptible to hypoxic and ischemic injury. DNA Cell Biol 16:311–321
18. Jang HH, Lee KO, Chi YH, Jung BG, Park SK, Park JH, Lee JR, Lee SS, Moon JC, Yun JW, Choi YO, Kim WY, Kang JS, Cheong GW, Yun DJ, Rhee SG, Cho MJ, Lee SY (2004) Two enzymes in one; two yeast peroxiredoxins display oxidative stress-dependent switching from a peroxidase to a molecular chaperone function. Cell 117:625–635
19. Jin D-Y, Chae HZ, Rhee SG, Jeang K-T (1997) Regulatory role for a novel human thioredoxin peroxidase in NF-kappaB activation. J Biol Chem 272:30952–30961
20. Kato S, Shimoda M, Watanabe Y, Nakashima K, Takahashi K, Ohama E (1996) Familial amyotrophic lateral sclerosis with a two base pair deletion in superoxide dismutase 1 gene: multisystem degeneration with intracytoplasmic hyaline inclusions in astrocytes. J Neuropathol Exp Neurol 55:1089–1101
21. Kato S, Hayashi H, Nakashima K, Nanba E, Kato M, Hirano A, Nakano I, Asayama K, Ohama E (1997) Pathological characterization of astrocytic hyaline inclusions in familial amyotrophic lateral sclerosis. Am J Pathol 151:611–620
22. Kato S, Funakoshi H, Nakamura T, Kato M, Nakano I, Hirano A, Ohama E (2003) Expression of hepatocyte growth factor and c-Met in the anterior horn cells of the spinal cord in the patients with amyotrophic lateral sclerosis (ALS): immunohistochemical studies on sporadic ALS and familial ALS with superoxide dismutase 1 gene mutation. Acta Neuropathol 106:112–120
23. Kato S, Shaw P, Wood-Allum C, Leigh PN, Show C (2003) Amyotrophic lateral sclerosis. In: Dickson D (ed) Nerodegeneration: the molecular pathology of dementia and movement disorders. ISN Neuropath Press, Basel, pp 350–368
24. Kato S, Saeki Y, Aoki M, Nagai M, Ishigaki A, Itoyama Y, Kato M, Asayama K, Awaya A, Hirano A, Ohama E (2004) Histological evidence of redox system breakdown caused by superoxide dismutase 1 (SOD1) aggregation is common to SOD1-mutated motor neurons in humans and animal models. Acta Neuropathol 107:149–158
25. Kato T, Hirano A, Kurland LT (1987) Asymmetric involvement of the spinal cord involving both large and small anterior horn cells in a case of familial amyotrophic lateral sclerosis. Clin Neuropathol 6:67–70
26. Koo KH, Lee S, Jeong SY, Kim ET, Kim HJ, Kim K, Song K, Chae HZ (2002) Regulation of thioredoxin peroxidase activity by c-terminal truncation. Arch Biochem Biophys 397:312–318
27. Kosower NS, Kosower EM (1978) The glutathione status of cells. Int Rev Cytol 54:109–160
28. Kurland LT, Mulder DW (1955) Epidemiologic investigations of amyotrophic lateral sclerosis. II. Familial aggregations indicative of dominant inheritance. Neurology 5:182–196, 249–268
29. Matsumoto A, Okado A, Fujii T, Fujii J, Egashira M, Niikawa N, Taniguchi N (1999) Cloning of the peroxiredoxin gene family in rats and characterization of the fourth member. FEBS Lett 443:246–250
30. Meister A, Anderson ME (1983) Glutathione. Annu Rev Biochem 52:711–760
31. Mu ZM, Yin XY, Prochownik EV (2002) Pag, a putative tumor suppressor, interacts with the myc box II domain of c-myc and selectively alters its biological function and target gene expression. J Biol Chem 277:43175–43184
32. Nagai M, Aoki M, Miyoshi I, Kato M, Pasinelli P, Kasai N, Brown RH Jr, Itoyama Y (2001) Rats expressing human cytosolic copper-zinc superoxide dismutase transgenes with amyotrophic lateral sclerosis: associated mutations develop motor neuron disease. J Neurosci 21:9246–9254
33. Nakano I, Hirano A, Kurland LT, Mulder DW, Holley PW, Saccomanno G (1984) Familial amyotrophic lateral sclerosis. Neuropathology of two brothers in American "C" family. Neurol Med (Tokyo) 20:458–471
34. Neumann CA, Krause DS, Carman CV, Das S, Dubey DP, Abraham JL, Bronson RT, Fujiwara Y, Orkin SH, Van Etten RA (2003) Essential role for the peroxiredoxin prdx1 in erythrocyte antioxidant defence and tumour suppression. Nature 424:561–565
35. Sen CK, Packer L (1996) Antioxidant and redox regulation of gene transcription. FASEB J 10:709–720
36. Shibata N, Hirano A, Kobayashi M, Siddique T, Deng HX, Hung WY, Kato T, Asayama K (1996) Intense superoxide dismutase-1 immunoreactivity in intracytoplasmic hyaline inclusions of familial amyotrophic lateral sclerosis with posterior column involvement. J Neuropathol Exp Neurol 55:481–490
37. Sun W, Funakoshi H, Nakamura T (2002) Overexpression of HGF retards disease progression and prolongs life span in a transgenic mouse model of ALS. J Neurosci 22:6537–6548
38. Takahashi K, Nakamura H, Okada E (1972) Hereditary amyotrophic lateral sclerosis. Histochemical and electron microscopic study of hyaline inclusions in motor neurons. Arch Neurol 27:292–299
39. Wood ZA, Poole LB, Karplus PA (2003) Peroxiredoxin evolution and the regulation of hydrogen peroxide signaling. Science 300:650–653

Neuropathology 2005; **25**, 365–370

Workshop: Recent Advances in Motor Neuron Disease

Development of a rat model of amyotrophic lateral sclerosis expressing a human *SOD1* transgene

Masashi Aoki,[1] Shinsuke Kato,[2] Makiko Nagai[1] and Yasuto Itoyama[1]

[1]Department of Neurology, Tohoku University School of Medicine, Sendai, and [2]Department of Neuropathology, Institute of Neurological Sciences, Faculty of Medicine, Tottori University, Yonago, Japan

Mutations in copper–zinc superoxide dismutase gene (*SOD1*) have been linked to some familial cases of ALS. We report here that rats that express a human *SOD1* transgene with two different ALS-associated mutations (G93A and H46R) develop striking motor neuron degeneration and paralysis. By comparing the two transgenic rats with different *SOD1* mutations, we demonstrate that the time course in these rats was similar to human *SOD1*-mediated familial ALS. As in the human disease and transgenic ALS mice, pathological analysis shows selective loss of motor neurons in the spinal cords of these transgenic rats. In addition, typical neuronal Lewy body-like hyaline inclusions as well as astrocytic hyaline inclusions identical to those in human familial ALS are observed in the spinal cords. The larger size of this rat model as compared with the ALS mice will facilitate studies involving manipulations of spinal fluid (implantation of intrathecal catheters for chronic therapeutic studies; CSF sampling) and spinal cord (e.g., direct administration of viral- and cell-mediated therapies).

Key words: astrocytic hyaline inclusions, amyotrophic lateral sclerosis, Lewy body-like hyaline inclusions, mutation, rat, *SOD1*, transgenic.

INTRODUCTION

ALS is a fatal neurodegenerative disease caused by the selective death of motor neurons.[1] Approximately 10% of the cases of ALS are inherited, usually as an autosomal dominant trait. In 25% of familial cases, the disease is caused by mutations in the gene encoding cytosolic copper–zinc superoxide dismutase (*SOD1*).[2,3] Nearly 100 different mutations in the *SOD1* gene have been identified in familial ALS.[4] Why the mutations cause motor neuron degeneration has not been fully elucidated.

In familial ALS kindred with mutations in the *SOD1* gene, the age of onset of weakness varies greatly but the duration of illness appears to be characteristic to each mutation. For example, in patients with the L84V mutation, the average life expectancy is less than 1.5 years after the onset of symptoms,[5,6] whereas patients harboring the H46R mutation have an average life expectancy of 18 years after the disease onset.[2,7] In view of the evidence supporting the idea that familial ALS variants of *SOD1* enzymes acquire toxic properties, the variations in the duration of illness in different kindred might arise because each mutation imparts different degrees of toxicity to the mutant protein.[8]

To date, several *SOD1* mutants of transgenic mice have been generated.[9–12] These mice exhibit the ALS-like clinical features and have importantly advanced our understanding of the pathogenesis of neuronal cell death induced by mutant SOD1 protein. They have also facilitated therapeutic trials. However, some types of experimental manipulations have been difficult in the ALS mice because of their innate size limitations. It has been almost impossible, for example, to analyze CSF from the ALS mice, even at single time points. It has also been very difficult to use therapies that involve administration of compounds into the CSF. There is only a single report of pump-mediated delivery of therapies to the CSF of the ALS mice, and that approach was intraventricular rather than intrathecal;[13] it is likely that intrathecal administration will produce significantly better therapeutic levels of compounds at the spinal cord level than will the intraventricular approach.[14] It has also been difficult to obtain sufficient tissue to perform extensive biochemical analyzes, such as investigations of post-transcriptional modifications of proteins like SOD1 itself during disease progression. For these reasons and in order

Correspondence: Masashi Aoki MD, PhD, Department of Neurology, Tohoku University School of Medicine, Seiryo-machi, Sendai 980-8574, Japan. Email: aokim@mail.tains.tohoku.ac.jp

Received 1 December 2004; accepted 8 December 2004.

to reproduce the different degrees of toxicity to the mutant protein by mutations, we have developed a rat model of ALS by expressing a human *SOD1* transgene with two ALS-associated mutations: H46R and G93A.[15]

CONSTRUCTION OF TRANSGENIC MICE EXPRESSING MUTANT HUMAN *SOD1*

We elected to make transgenic rats with two mutations in the *SOD1* genes: histidine 46 to arginine (H46R) and glycine 93 to alanine (G93A). In patients we have encountered with these mutations, the phenotypes are quite different. For H46R patients, progression is extremely slow[2,7] whereas patients with the $SOD1^{G93A}$ mutation demonstrate a more fulminant, classical clinical course.[16] Moreover, the transgenic ALS mouse with this G93A mutation has been widely distributed and studied throughout the world.[9]

To generate the transgenic rats with the H46R and the G93A mutations, we first obtained human genomic PAC clones encompassing the entire human *SOD1* gene; we then subcloned this gene within an 11.5 kb *Eco*RI–*Bam*HI fragment. Site-directed mutagenesis was used to generate clones with either the H46R or the G93A mutations. The mutated 11.5 kb *Eco*RI–*Bam*HI fragments were microinjected into fertilized eggs from Sprague Dawley (SD) rats (Japan SLC, Hamamatsu, Japan). Twenty-five potential transgenic H46R pups were obtained. From these, five founders with the H46R mutant transgene were identified using PCR and Southern blotting. Fifty-two potential transgenic G93A pups were obtained. From these, seven founders with the G93A mutant transgene were identified. Levels of accumulated mutant *SOD1* were measured for almost all founders by quantitative protein immunoblotting of spinal cord extracts using antibody against a peptide sequence that is identical in human and rat *SOD1*.

The transgenic rats expressing the higher levels of each human *SOD1* mutant (lines G93A-39 and H46R-4) have developed motor neuron disease (Fig. 1). Clinically apparent weakness, denoted by dragging of one hindlimb without limb tremor, was evident somewhat later. The mean age of onset of this clinical weakness for the G93A-39 line was 122.9 days ($n = 14$); for the H46R-4 line, the age of onset was 171.7 days ($n = 11$) (Fig. 1). Simultaneously with the onset of clinical weakness, the affected rats showed prominent weight loss. Although the initial clinical manifestation of weakness was unilateral leg paralysis, this progressed and became bilateral in both lines of rats. In the early stages of the illness, another distinctive abnormality was increased tone in the tail musculature, resulting in an elevated, segmentally spastic tail posture. As the disease progressed, the rats exhibited marked muscle wasting in the hindlimbs, typically dragging themselves about the

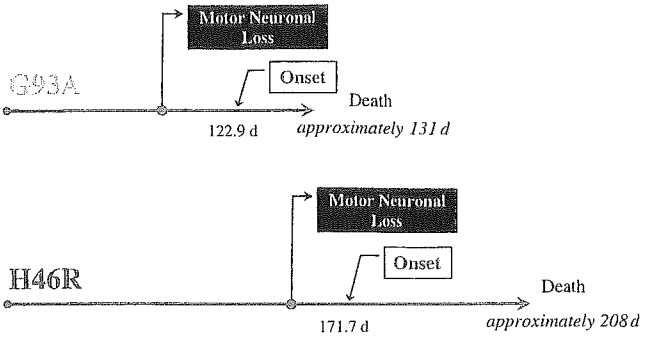

Fig. 1 Progression of mutant superoxide dismutase-mediated disease. From the presymptomatic stage, the anterior horns of the same rats revealed decreased numbers of large, multipolar neuronal cells (motor neurons) with proliferation of small non-neuronal cells with morphological characteristics of astrocytes and microglia. The ages of onset and death for the G93A-39 and H46R-4 rats are indicated.

Fig. 2 An affected transgenic rat from the H46R-4 line demonstrates hindlimb weakness and abnormal posturing with segmental spasticity of the tail.

cage using the forelimbs (Fig. 2). Thereafter, the forelimbs also became weak, in association with further weight loss. At end-stage, the affected rats could not drink water and died. The mean duration of the disease in the G93A-39 and H46R-4 lines were 8.3 days ($n = 14$) and 37.2 days ($n = 11$), respectively. All rats were handled according to approved animal protocols in our institution.

HISTOPATHOLOGICAL AND IMMUNOHISTOCHEMICAL ANALYZES

The H46R and G93A transgenic rats exihibit the same histopathological changes as those in human familial ALS patients with *SOD1* gene mutations. Therefore, at present,

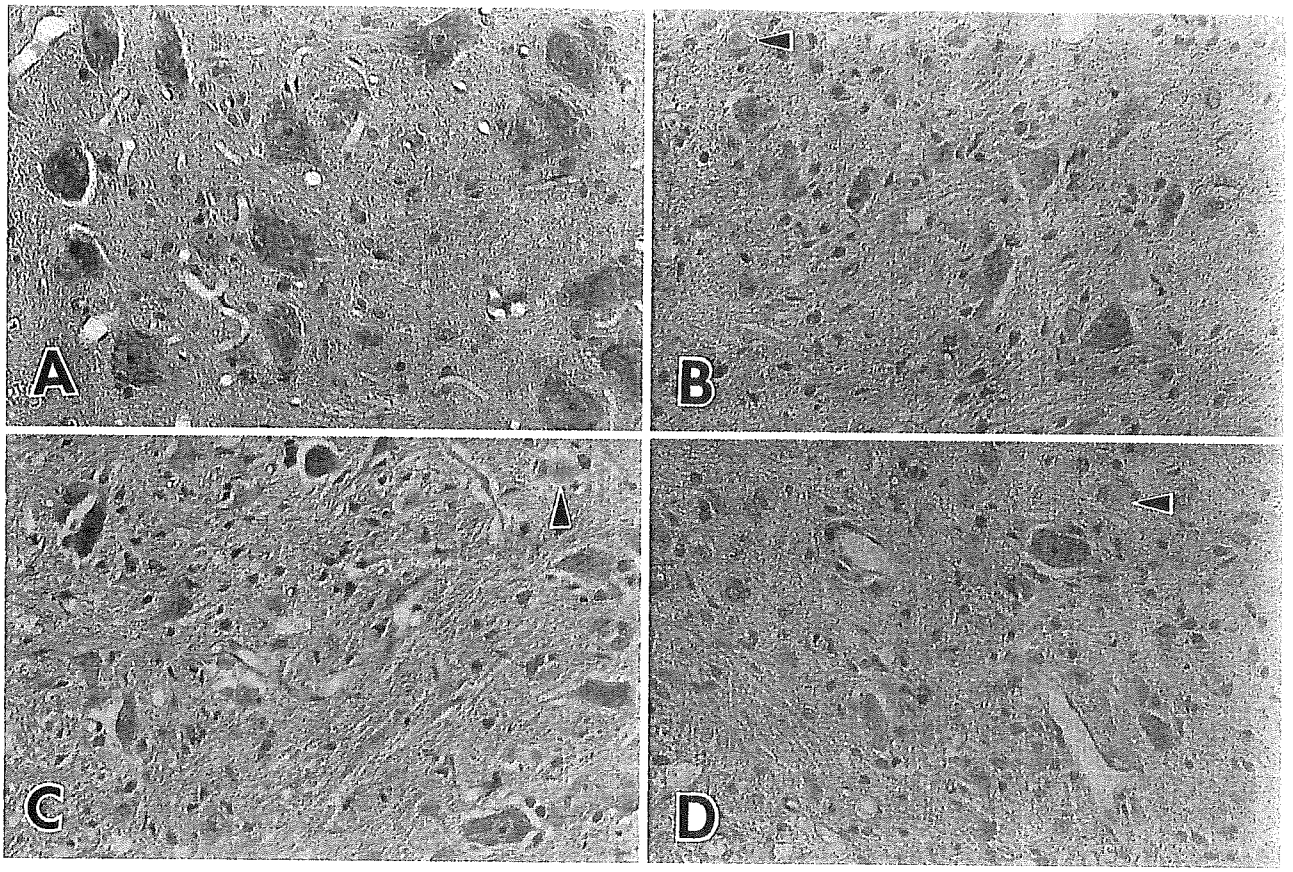

Fig. 3 Histological and histopathological findings in H46R transgenic rats and littermate. (A) The anterior horn of the spinal cord in littermate rat at the age of 160 days: approximately 15 normal anterior horn cells can be observed. (B) The anterior horn of the spinal cord in H46R transgenic rat at the age of 160 days: approximately six anterior horn cells can be counted in the H46R transgenic rat of this age, that is, the number of the anterior horn cells is decreased with astrocytic gliosis, histopathologically, in comparison with the littermate at the same age in (A). A core and halo-type astrocytic hyaline inclusion (Ast-HI) is evident (arrowhead). (C) The anterior horn of the spinal cord in the H46R transgenic rat at the age of 170 days: the histopathological finding of this age reveals loss of the anterior horn cells and gliosis of the spinal cords. A core and halo-type Ast-HI can be observed (arrowhead). (D) The anterior horn of the spinal cord in the H46R transgenic rat at the age of 200 days corresponding to the end-stage: approximately two anterior horn cells can be recognized at this terminal stage; the H46R rats of the terminal stage show severe loss of the anterior horn cells with gliosis of the spinal cords histopathologically compatible with those in ALS patients with clinical courses of over 5 years. A core and halo-type Ast-HI can be seen (arrowhead). As in human ALS patients, small-sized remaining anterior horn cells that appear to be normal are also observed throughout the disease courses in H46R transgenic rats (B–D) ((A–D): HE; magnification: ×400).

we think that the H46R and G93A transgenic rats are neuropathologically most optimal as animal models of familial ALS with the *SOD1* mutations. An essential histopathological finding of the spinal cords in ALS patients is loss of the anterior horn cells.[17] When we focus on the anterior horn cells of the spinal cords in both H46R and G93A transgenic rats, the anterior horn cells of the H46R and G93A transgenic rats are decreased before the development of clinical motor deficits. At the level of cellular pathology, the H46R and G93A transgenic rats develop Lewy body-like hyaline inclusions (LBHI) in neurons and astrocytes, which are morphological hallmarks of certain human familial ALS patients with the *SOD1* gene mutations.[17–20]

With respect to the histopathological aspects of H46R transgenic rats, the number of the anterior horn cells of the 160-day-old H46R rats that exhibit hind limb paresis is decreased with astrocytic gliosis in the spinal cords in comparison with the littermates at the same age (Fig. 3A,B). At 170 days of age when the H46R rats indicate hindlimb paraplegia sometimes associated with forelimb weakness, the histopathological finding of this clinical stage reveals more severe loss of the anterior horn cells and gliosis of the spinal cords in comparison with that of 160 days of age (Fig. 3B,C). At 200 days of age corresponding to the end-stage when the H46R rats clinically display quadriplegia or a moribund state, the H46R rats of this end-stage show severe loss of the anterior horn cells with gliosis of the spi-

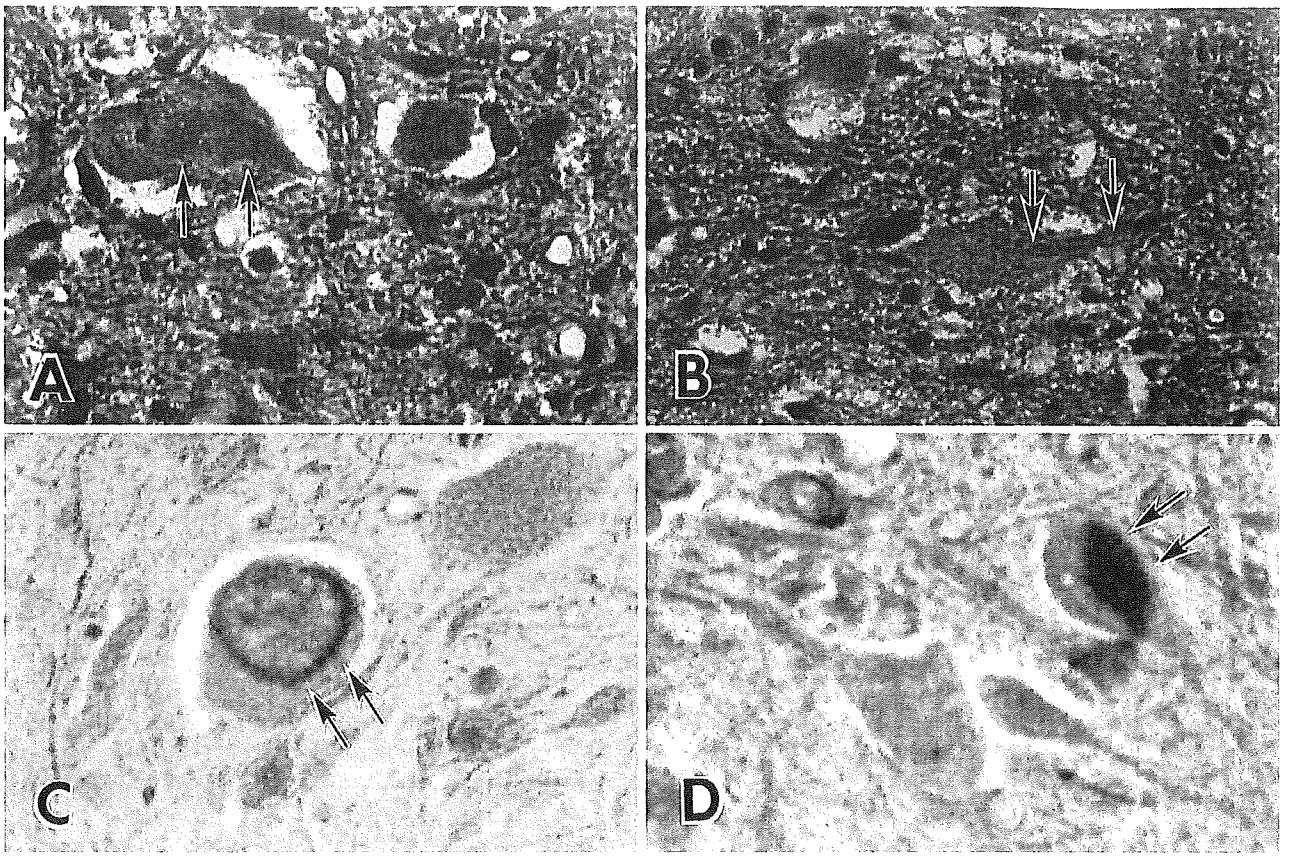

Fig. 4 Neuronal Lewy body-like hyaline inclusions (LBHI) in H46R transgenic rats. (A) A typical intracytoplasmic neuronal LBHI with a core and halo is indicated by double arrows (HE; magnification: ×820). (B) A neuronal LBHI with a core and halo is located from the cytoplasm to the dendrite (double arrows) (HE; magnification: ×820). (C) An intracytoplasmic LBHI is positive for SOD1; only the periphery of the neuronal LBHI is strongly immunostained (double arrows) (Immunostaining for SOD1; magnification: ×820). (D) An intracytoplasmic LBHI is diffusely immunostained (double arrows) (Immunostaining for SOD1; magnification: ×820). (Figure 4C is from Kato *et al.*[18] and reproduced with permission from *Acta Neuropathol*).

nal cords histopathologically compatible with those in ALS patients with clinical courses of over 5 years (Fig. 3D). As in human ALS patients, small-sized remaining anterior horn cells that appear to be normal in HE preparations are also observed throughout the disease courses in H46R and G93A transgenic rats (Fig. 3A–D).

As for the cell-pathological and immunohistochemical aspects, the rodent familial ALS model of these rats has the other important cellular pathological finding compatible with that in human familial ALS patients with the *SOD1* gene mutations; typical intracytoplasmic neuronal LBHI are observed in the remaining anterior horn cells of the spinal cords in the rat model of familial ALS. Cell-pathologically, the intracytoplasmic neuronal LBHI in the rat model of ALS are identical to those in human familial ALS. In both the rat model and human familial ALS, neuronal LBHI are formed not only in the cytoplasm but also in dendrites (Fig. 4A,B). Immunohistochemically, as in human mutant *SOD1*-mediated familial ALS,[17,19,20] the neuronal LBHI in the rat model of ALS with the H46R and G93A are positive for SOD1 (Fig. 4C,D). The reaction product deposits of the antibody against SOD1 are generally restricted to the periphery of the LBHI that show eosinophilic cores with palor peripheral halos in HE preparations (Fig. 4C). The immunostaining in intracytoplasmic and intradendtritic ill-defind LBHI is distributed throughout each of the inclusions (Fig. 4D). The rat model of ALS with the H46R and G93A also develops astrocytic hyaline inclusions (Ast-HI) that are identical structures observed in human long-term surviving familial ALS patients with the *SOD1* gene mutation.[17,19,20] In HE preparations, similarly in neuronal LBHI, Ast-HI are eosinophilic (Fig. 5A) or slightly pale inclusions and sometimes show an eosinophilic core with palor peripheral halos (Fig. 3B–D). The Ast-HI are generally round to oval and sometimes sausage-like in shape. As in neuronal LBHI, immunohistochemically, Ast-HI are intensely immunostained by the antibody against SOD1 (Fig. 5B).

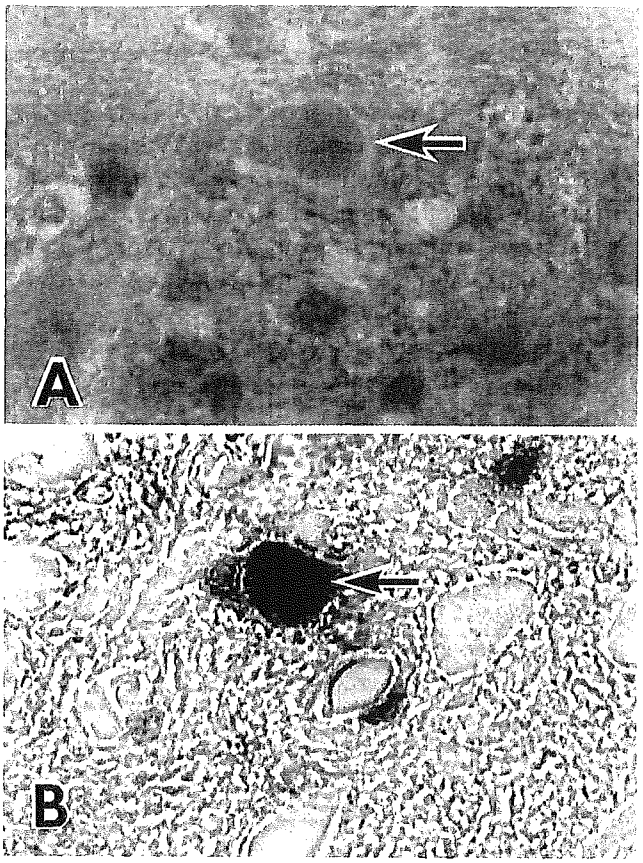

Fig. 5 Astrocytic hyaline inclusions (Ast-HI) in H46R transgenic rats. (A) Typical eosinophilic Ast-HI can be seen (arrow) (HE; magnification: ×1200). (B) An Ast-HI is strongly positive for SOD1 (arrow) (Immunostaining for SOD1; magnification: ×1200).

DISCUSSION

We have established lines of rats that express transgenes for mutant SOD1 protein with two different ALS-associated mutations: H46R and G93A. Rats with the highest transgene copy numbers and levels of expression of the mutant protein develop a paralytic disorder characterized by fulminant motor neuron death accompanied by astrogliosis and microgliosis. Particularly striking in our data is not only the earlier onset of the G93A disease but also the much more rapid course in the G93A-39 (8 days) as compared to the H46R-4 (37 days) rats. We do not understand the basis for this difference in rate of disease progression, but we note those factors determining the time course in these rats are likely to be relevant to human mutant *SOD1*-mediated familial ALS. The human H46R cases also progress very slowly, with a mean survival of 16.8 ± 6.8 years.[2,7] By contrast, the mean survival of the G93A cases in one report was 2.2 ± 1.5 years.[16] Although it is tempting to speculate that this shorter disease duration is a consequence of the higher retained dismutation activity in the G93A-39 line, we cannot firmly conclude this.

A transgenic rat model of human ALS will offer several advantages with respect to the existing transgenic mouse ALS models.[15,21] Given its larger size, it will facilitate all studies that entail CSF analysis and, in particular, those that entail multiple, serial manipulations of CSF in the same animal. Thus, it will be possible in this model to obtain adequate CSF for conventional biochemical studies as well as analyzes of small molecules and even DNA/RNA species that may distinguish the ALS from the wild-type CSF. Moreover, this model should be ideal for administration of therapies via chronic intrathecal pumps, a strategy that has been employed recently in human ALS clinical trials.[22] Another advantage of the ALS rats is that they can tolerate some forms of immunosuppressive therapy that are problematic in mice, such as cyclosporine A. This point arises in the context of an emerging interest in possible strategies to use implanted neural stem cells as therapy in ALS. It should now be possible to achieve appropriate immunosuppression in the ALS rats to allow survival of implanted cells and hence determine the efficacy of this approach. As a corollary, we also note that the larger size of the rat spinal cord will facilitate delivery of cells to the target spinal cord regions.

CONCLUSIONS

We have established lines of rats that express transgenes for mutant SOD1 protein with two different ALS-associated mutations: H46R and G93A. As in the human disease and transgenic ALS mice, pathological analysis demonstrates selective loss of motor neurons in the spinal cords of these transgenic rats. In addition, typical neuronal LBHI as well as Ast-HI identical to those in human familial ALS are observed in the spinal cords of the rats. Therefore, at present, we think that the H46R and G93A transgenic rats are neuropathologically most optimal as animal models of familial ALS with the *SOD1*-mutations.

ACKNOWLEDGMENTS

This work was supported by Grant-in-Aid from the Ministry of Health, Labour and Welfare (MA, SK, YI) and Haruki ALS Research Foundation (MA, YI).

REFERENCES

1. Brown RH Jr. Superoxide dismutase in familial amyotrophic lateral sclerosis models for gain of function. *Curr Opin Neurobiol* 1995; **5**: 841–846.
2. Aoki M, Ogasawara M, Matsubara Y *et al.* Mild ALS in Japan associated with novel SOD mutation. *Nat Genet* 1993; **5**: 323–324.

3. Rosen DR, Siddique T, Patterson D *et al.* Mutations in Cu/Zn superoxide dismutase gene are associated with familial amyotrophic lateral sclerosis. *Nature* 1993; **362**: 59–62.
4. Andersen PM, Sims KB, Xin WW *et al.* Sixteen novel mutations in the Cu/Zn superoxide dismutase gene in amyotrophic lateral sclerosis: a decade of discoveries, defects and disputes. *Amyotroph Lateral Scler Other Motor Neuron Disord* 2003; **4**: 62–73.
5. Aoki M, Abe K, Houi K *et al.* Variance of age at onset in a Japanese family with amyotrophic lateral sclerosis associated with a novel Cu/Zn superoxide dismutase mutation. *Ann Neurol* 1995; **37**: 676–679.
6. Deng HX, Tainer JA, Mitsumoto H *et al.* Two novel SOD1 mutations in patients with familial amyotrophic lateral sclerosis. *Hum Mol Genet* 1995; **4**: 1113–1116.
7. Aoki M, Ogasawara M, Matsubara Y *et al.* Familial amyotrophic lateral sclerosis (ALS) in Japan associated with H46R mutation in Cu/Zn superoxide dismutase gene: a possible new subtype of familial ALS. *J Neurol Sci* 1994; **126**: 77–83.
8. Aoki M, Abe K, Itoyama Y. Molecular analyses of the Cu/Zn superoxide dismutase gene in patients with familial amyotrophic lateral sclerosis (ALS) in Japan. *Cell Mol Neurobiol* 1998; **18**: 639–647.
9. Gurney ME, Pu H, Chiu AY *et al.* Motor neuron degeneration in mice that express a human Cu,Zn superoxide dismutase mutation. *Science* 1994; **264**: 1772–1775.
10. Wong PC, Pardo CA, Borchelt DR *et al.* An adverse property of a familial ALS-linked SOD1 mutation causes motor neuron disease characterized by vacuolar degeneration of mitochondria. *Neuron* 1995; **14**: 1105–1116.
11. Bruijn LI, Becher MW, Lee MK *et al.* ALS-linked SOD1 mutant G85R mediates damage to astrocytes and promotes rapidly progressive disease with SOD1-containing inclusions. *Neuron* 1997; **18**: 327–338.
12. Wang J, Xu G, Gonzales V *et al.* Fibrillar inclusions and motor neuron degeneration in transgenic mice expressing superoxide dismutase 1 with a disrupted copper-binding site. *Neurobiol Dis* 2002; **10**: 128–138.
13. Li M, Ona VO, Guegan C *et al.* Functional role of caspase-1 and caspase-3 in an ALS transgenic mouse model. *Science* 2000; **288**: 335–339.
14. Gurney ME, Tomasselli AG, Heinrikson RL. Stay the executioner's hand. *Science* 2000; **288**: 283–284.
15. Nagai M, Aoki M, Miyoshi I *et al.* Rats expressing human cytosolic copper-zinc superoxide dismutase transgenes with amyotrophic lateral sclerosis: associated mutations develop motor neuron disease. *J Neurosci* 2001; **21**: 9246–9254.
16. Cudkowicz M, McKenna-Yasek D, Sapp P *et al.* Epidemiology of SOD1mutations in amyotrophic lateral sclerosis. *Ann Neurol* 1997; **41**: 210–212.
17. Kato S, Shaw P, Wood-Allum C, Leigh PN, Show C. Amyotrophic lateral sclerosis. In: Dickson D (ed.) *Nerodegeneration: the Molecular Pathology of Dementia and Movement Disorders*. Basel: ISN Neuropath Press, 2003; 350–368.
18. Kato S, Saeki Y, Aoki M *et al.* Histological evidence of redox system breakdown caused by superoxide dismutase 1 (SOD1) aggregation is common to SOD1-mutated motor neurons in humans and animal models. *Acta Neuropathol* 2004; **107**: 149–158.
19. Kato S, Saito M, Hirano A, Ohama E. Recent advances in research on neuropathological aspects of familial amyotrophic lateral sclerosis with superoxide dismutase 1 gene mutations: neuronal Lewy body-like hyaline inclusions and astrocytic hyaline inclusions. *Histol Histopathol* 1999; **14**: 973–989.
20. Kato S, Takikawa M, Nakashima K *et al.* New consensus research on neuropathological aspects of familial amyotrophic lateral sclerosis with superoxide dismutase 1 (SOD1) gene mutations: inclusions containing SOD1 in neurons and astrocytes. *Amyotroph Lateral Scler Other Motor Neuron Disord* 2000; **1**: 163–184.
21. Howland DS, Liu J, She Y *et al.* Focal loss of the glutamate transporter EAAT2 in a transgenic rat model of SOD1 mutant-mediated amyotrophic lateral sclerosis (ALS). *Proc Natl Acad Sci USA* 2002; **99**: 1604–1609.
22. Mitsumoto H, Gordon P, Kaufmann P, Gooch CL, Przedborski S, Rowland LP. Randomized control trials in ALS: lessons learned. *Amyotroph Lateral Scler Other Motor Neuron Disord* 2004; **5** (Suppl. 1): 8–13.

Journal of Neuroscience Research 82:63–70 (2005)

Motoneuron Degeneration After Facial Nerve Avulsion Is Exacerbated in Presymptomatic Transgenic Rats Expressing Human Mutant Cu/Zn Superoxide Dismutase

Ken Ikeda,[1,2] Masashi Aoki,[3] Yoko Kawazoe,[1] Tsuyoshi Sakamoto,[1] Yuichi Hayashi,[1] Aya Ishigaki,[3] Makiko Nagai,[3] Rieko Kamii,[3] Shinsuke Kato,[4] Yasuto Itoyama,[3] and Kazuhiko Watabe[1]*

[1]Department of Molecular Neuropathology, Tokyo Metropolitan Institute for Neuroscience, Tokyo, Japan
[2]Department of Neurology, PL Tokyo Health Care Center, Tokyo, Japan
[3]Department of Neurology, Tohoku University Graduate School of Medicine, Sendai, Japan
[4]Department of Neuropathology, Institute of Neurological Sciences, Faculty of Medicine, Tottori University, Yonago, Japan

We investigated motoneuron degeneration after proximal nerve injury in presymptomatic transgenic (tg) rats expressing human mutant Cu/Zn superoxide dismutase (SOD1). The right facial nerves of presymptomatic tg rats expressing human H46R or G93A SOD1 and their non-tg littermates were avulsed, and facial nuclei were examined at 2 weeks postoperation. Nissl-stained cell counts revealed that facial motoneuron loss after avulsion was exacerbated in H46R- and G93A-tg rats compared with their non-tg littermates. The loss of motoneurons in G93A-tg rats after avulsion was significantly greater than that in H46R-tg rats. Intense cytoplasmic immunolabeling for SOD1 in injured motoneurons after avulsion was demonstrated in H46R- and G93A-tg rats but not in their littermates. Facial axotomy did not induce significant motoneuron loss nor enhance SOD1 immunoreactivity in these tg rats and non-tg littermates at 2 weeks postoperation, although both axotomy and avulsion elicited intense immunolabeling for activating transcription factor-3, phosphorylated c-Jun, and phosphorylated heat shock protein 27 in injured motoneurons of all these animals. The present data indicate the increased vulnerability of injured motoneurons after avulsion in the presymptomatic mutant SOD1-tg rats. © 2005 Wiley-Liss, Inc.

Key words: axotomy; facial nerve; amyotrophic lateral sclerosis; ALS; mutant Cu/Zn superoxide dismutase; SOD1; transgenic rat

Since the discovery of the mutation of Cu/Zn superoxide dismutase (SOD1) in patients with familial amyotrophic lateral sclerosis (ALS) and the development of transgenic (tg) mice and rats expressing human mutant SOD1 that show clinicopathological characteristics comparable to human familial ALS, the mutant SOD1-tg animals have been the most widely used experimental models for elucidating the pathomechanism of and the therapeutic approach for familial ALS as well as sporadic ALS (Cleveland and Rothstein, 2001). Although the precise mechanism of motoneuron degeneration in mutant SOD1-tg animals is largely unknown, the mutant SOD1 is thought to have a gain of toxic function (Cleveland and Rothstein, 2001). In another animal model of motoneuron degeneration, peripheral nerve avulsion exhibits extensive loss of motoneurons in adult rats (Søreide, 1981; Wu, 1993; Koliatsos et al., 1994; Watabe et al., 2000; Sakamoto et al., 2000, 2003a,b; Ikeda et al., 2003; Moran and Graeber, 2004). The mechanism of motoneuron degeneration after avulsion also remains unclear, but peroxinitrite-mediated oxidative damage and perikaryal accumulation of phosphorylated neurofilaments have been demonstrated in injured motoneurons after avulsion (Martin et al., 1999). Both of these pathological features have also been shown in

Contract grant sponsor: Ministry of Education, Culture, Sports, Science and Technology, Japan; Contract grant sponsor: Research on Specific Diseases, Health Sciences Research Grants, Ministry of Health, Labor and Welfare, Japan; Contract grant sponsor: Research on Psychiatric and Neurological Diseases and Mental Health, H16-kokoro-017, Ministry of Health, Labor and Welfare, Japan.

*Correspondence to: Kazuhiko Watabe, MD, PhD, Department of Molecular Neuropathology, Tokyo Metropolitan Institute for Neuroscience, 2-6 Musashidai, Fuchu, Tokyo 183-8526, Japan.
E-mail: kazwtb@tmin.ac.jp

Received 6 April 2005; Revised 31 May 2005; Accepted 30 June 2005

Published online 17 August 2005 in Wiley InterScience (www.interscience.wiley.com). DOI: 10.1002/jnr.20621

© 2005 Wiley-Liss, Inc.